AD NUMBER

AD809185

NEW LIMITATION CHANGE

TO

Approved for public release, distribution unlimited

FROM

Distribution authorized to U.S. Gov't. agencies and their contractors; Administrative/Operational Use; Nov 1966. Other requests shall be referred to Air Force Aero Propulsion Lab., Wright-Patterson AFB, OH 45433.

AUTHORITY

AFAPL ltr, 12 Apr 1972

AFAPL-TR-66-90

AN ANALYTICAL METHOD OF DETERMINING GENERAL DOWNWASH FLOW FIELD PARAMETERS FOR V/STOL AIRCRAFT

DAVID J. HOHLER

TECHNICAL REPORT AFAPL-TR-66-90

NOVEMBER 1966

AIR FORCE AERO PROPULSION LABORATORY
RESEARCH AND TECHNOLOGY DIVISION
AIR FORCE SYSTEMS COMMAND
WRIGHT-PATTERSON AIR FORCE BASE, OHIO

AFAPL-TR-66-90

AN ANALYTICAL METHOD OF DETERMINING GENERAL DOWNWASH FLOW FIELD PARAMETERS FOR V/STOL AIRCRAFT

DAVID J. HOHLER

FOREWORD

This report presents the results of a study conducted by Mr. David J. Hobler concerning a means of determining the general downwash flow field parameters for various types of V/STOL aircraft. It consists of a study of past experimental data generated by both the government and private industry and an analysis of certain theoretical approaches used in an attempt to achieve data correlation.

This work was conducted under Project No. 8174, Task No. 817401. The research covered in this report was accomplished from April 1966 to August 1966. This report was submitted by the author in August 1966.

This technical report has been reviewed and is approved.

A. Vasiloff

A. VASILOFF
Technical Area Manager
Ground Support Branch
Support Technology Division

ABSTRACT

This report presents a method of analytically determining the general downwash flow field parameters of various types of V/STOL aircraft. The basic difference between the operation of V/STOL aircraft and conventional aircraft is their method of take-off and landing. During these operations, V/STOL aircraft produce high downwash air velocities that impinge and spread out over the surface of the ground. Depending on the size, type, and number of engines on the aircraft, this downwash can cause damage to nearby aircraft, equipment, or personnel. Past theoretical methods based on incompressible flow theory have been unsuccessful in establishing a means of computing this downwash flow field. A combined method, however, of proven experimental data and certain analytical approaches have yielded a useful means of predicting the general downwash flow field parameters. This report presents these approaches and demonstrates their usefulness.

TABLE OF CONTENTS

SECTION		PAGE
I	INTRODUCTION	1
II	OVERALL FLOW FIELD ANALYSIS	2
	1. General Flow Field Description	2
	2. Flow Field Areas of Analysis	2
	3. Calculation Procedures	4
	a. Free Jet Region (Region I)	4
	b. Turning Region (Region II)	6
	c Wall Jet Region (Region III)	13
	4. General Considerations	15
	5. Conclusions and Recommendations	15
III	GROUNDWASH ANALYSIS	21
	1. General Flow Field Description	21
	a. Jet Aircraft Analysis	21
	b. Propeller - Rotor Aircraft Analysis	24
	2. General Considerations	29
	3. Conclusions and Recommendations	29
IV	SUMMARY OF V/STOL EXPERIMENTAL DATA	31
	1. Jet Nozzle Performance Data	31
	2. Rotor and Propeller Performance Data	32
	3. Near-Ground Operational Performance	42
	4. General V/STOL Engine Environment and Aircraft Performance Data	42
	5. Summary of V/STOL Aircraft Specifications	53
REFERENCES		60

ILLUSTRATIONS

FIGURE		PAGE
1.	Schematic of Nozzle Downwash Flow	3
2.	Axisymmetric Free Jet from a Circular Nozzle	5
3.	Center Line Velocity of Zones 1 and II of Region I	7
4.	Nozzle Center Line Static Pressure Ratio in the Turning Region	10
5.	Ground Static Pressure Ratio in Region II	11
6.	Ground Velocity Ratio in Region II	12
7.	Maximum Velocity of Flow in the Wall Jet Region	14
8.	Nomenclature for Zone B of Region III	16
9.	Reynolds Number for Region III	17
10.	Parameters a, b, and α Versus Reynolds Number	18
11.	Velocity Profiles for Zone B of the Wall Jet Region	19
12.	Maximum Ground Velocity at Various Distances from Jet Exit	23
13.	Variation in K From Equation 25 for Various Nozzle Exit Heights	25
14.	Maximum Ground Velocity at Various Distances From the Propeller Exit	26
15.	Variation in K of Equation 25 for Various Propeller Exit Heights	27
16.	Ground Dynamic Pressure Decay for Propeller or Rotor at H/D = 0.4	28
17.	Correlation of Theoretical and Experimental Data of Ground Dynamic Pressure Decay	30
18.	Dynamic Pressure Decay of a 1-Inch Circular Convergent Nozzle in Free Air	33
19.	Jet Wake Dynamic Pressure Degradation at the Exit Gas Temperatures	34
20.	Jet Wake Differential Temperature Degradation for a Circular Convergent Nozzle in Free Air	35
21.	Jet Wake Dynamic Pressure and Differential Temperature Survey for a Circular Convergent Nozzle	36
22.	Effect of Ground Plane on Jet Wake Degradation Characteristics for a Circular Nozzle	37

ILLUSTRATIONS (CONT'D)

FIGURE		PAGE
23.	Radial Variation of Local Dynamic Pressure over the Ground Plane for a Circular Nozzle (from Various References)	38
24.	Jet Wake Pressure Degradation at Various Nozzle Pressure Ratios for a Circular Nozzle	39
25.	Pressure Profiles over the Ground Plane (q_g/q_n) for a Circular Nozzle	40
26.	Differential Temperature Profiles (τ_g/τ_n) Adjacent to the Ground Plane for a Circular Nozzle	41
27.	Comparison Between Theoretical and Experimental Downwash Velocities for a Rotor in Free Air	43
28.	Dynamic Pressure Decay and Slipstream Profile of a Propeller and a Ducted Fan in Free Air	44
29.	Velocity Contour Map for a Rotor in Ground Effect and in Free Air	45
30.	Static Pressure Distribution for a Rotor 1.0 Radius Above Ground	46
31.	Ground Static Pressure for Various Rotor Heights	47
32.	Ground Velocity Profiles at Various Rotor Heights for Different Ground Stations	48
33.	Effect of Near-Ground Operation on a Single-Jet-Model Configuration	49
34.	Effect of Nozzle Height on Lift Losses for Various Circular Planform Plate Areas	49
35.	Induced Load on Several Planform Plates and Pressure Decay for Single and Multiple Jet Configurations in Free Air	50
36.	Variation in Lift of a Propeller or Rotor and a Ducted Fan near the Ground	51
37.	Effect of Ground on Various Aircraft Configurations and Types	52
38.	Aircraft Engine Downwash Environment	54
39.	Terrain Resistance to Overpressure	55
40.	Hovering and Cruise Performance	56
41.	STOL Performance - Takeoff Distance over a 50-Foot Obstacle	56
42.	Fuel Consumption in Hovering	57

SYMBOLS

a	exponent in wall jet, Equation 13, (See Figure 7)
A_e	exit area of duct, ft.^{2}
A_j	jet nozzle exit area, ft.^{2}
b	exponent in wall jet, Equation 14, (See Figure 7)
C	axial distance from nozzle to point of theoretical jet origin, ft.
D	diameter of the nozzle or ducted fan, or effective diameter of slipstream from free propeller or rotor (0.707 Dp), ft.
D_e	equivalent diameter of a single jet whose area equals the total area of the multiple jets, ft.
D_p	diameter of propeller or rotor, ft.
D_pL	disk loading, thrust / $\frac{\pi}{4} D_p 2$
h	distance above ground, ft.
H	height of nozzle or propeller exit above ground, ft.
h_f	height of aircraft fuselage off the gound, ft.
L	lift, lbs.
L_∞	lift, out of ground effect, lbs.
P	static pressure in the turning region, lbs/ft.^{2}
P_o	atmospheric pressure, lbs/ft.^{2}
P_{s_g}	local static pressure measured in the ground plane, lbs/ft^2
P_T	stagnation pressure, lbs/ft.^{2}
P_{t_g}	stagnation pressure at any specified point in the jet wake, lbs/ft.^{2}
$P_{t_{g\,max}}$	maximum stagnation pressure at any specified point on, or adjacent to, the ground plane, lb/ft.^{2}
P_{t_n}	stagnation pressure at the nozzle exit, lbs/ft.^{2}
$P_{t_{z\,max}}$	maximum stagnation pressure at any specified point in the jet wake, lbs/ft.^{2}

SYMBOLS (CONT'D)

q	downwash dynamic pressure, lbs/ft.^{2}
q_e	average exhaust exit dynamic pressures, lbs/ft.^{2}
q_g	local dynamic pressure at any specified point, on or adjacent to, the ground plane, $P_{t_g} - P_0$, lbs/ft.^{2}
q_{max}	maximum dynamic pressure along the ground surface at any radial distance from the downwash center line, lbs/ft.^{2}
q_n	average dynamic pressure at nozzle exit, $P_{t_n} - P_0$, lbs/ft.^{2}
q_z	local dynamic pressure at any specified point in the jet wake, $P_{t_z} - P_0$, lbs/ft.^{2}
$q_{z\ max}$	maximum dynamic pressure measured at any specified plane perpendicular to the Z axis, lbs/ft.^{2}
r	radial distance measured from the centerline of the jet nozzle, ducted fan, rotor or propeller, ft.
r_o	radius of outside of jet (Zones I and II in free jet region only), ft.
r_1	radius of core of air at $U = U_m$ (zone I in free jet region only), ft.
R	radius of nozzle or ducted fan or effective radius of slipstream from free propeller or rotor, ft.
R'	equivalent jet radius into turning region, ft.
R_p	radius of propeller or rotor, ft.
S	area of removable nozzle plate, ft.^{2}
t	time, hours
t_o	ambient temperature, °F
t_{t_g}	total temperature measured in the jet efflux over the gound plane, °F
t_{t_n}	total temperature at nozzle exit, °F
$t_{t_{z\ max}}$	maximum total temperature measured at any specified plane perpendicular to the Z axis, °F
T	jet nozzle thrust, lbs.
U	vertical velocity, ft/sec.
U_m	mean velocity required over initial flow area to produce given thrust, ft/sec.
U_{max}	maximum vertical velocity at a distance Z from the nozzle exit, ft./sec.

SYMBOLS (CONT'D)

v	velocity, ft/sec.
V	horizontal Velocity, ft/sec.
V_g	maximum radial velocity at a radial distance r from jet centerline equal to 2R', ft/sec.
V_o	mean induced velocity in plane of rotor or propeller, (V_o = 1/2 fully developed wake velocity), ft/sec.
V_w	local wake velocity (propeller or rotor), ft/sec.
V_{max}	maximum radial velocity at a radial distance r from the jet centerline, ft/sec.
W	total airplane weight, lbs.
W_f	fuel weight, lbs.
X	distance from nozzle core to any point in the mixing region, measured parallel to the X axis, ft.
X_g	radial distance along the ground measured from the center of the ground plane, ft.
Z	vertical distance from nozzle, ducted fan or propeller exit, ft.
α	term in wall jet expression, a function of Reynolds Number.
δ	height above the ground where $V = 1/2\ V_{max}$, ft. (see Fig. 8)
δ_m	height of the point of maximum velocity, ft.
ρ	density, (lbs/ft^2)
ν	kinematic viscosity of air (or fluid), ($ft^2/sec.$)
τ_g	differential temperature at any specified point on, or adjacent to, the ground plane, $t_g - t_o$, °F
τ_n	differential temperature at the nozzle exit, $t_n - t_o$, °F
τ_{zmax}	maximum differential temperature measured at any specified plane perpendicular to the Z axis, $t_{z\ max} - t_o$, °F

SECTION I

INTRODUCTION

The V/STOL aircraft differs from conventional aircraft in that the engine or engine slipstream is directed vertically downward to provide either a partial or complete vertical component of lift. This extra lift, in addition to any normal wing lift, allows the aircraft to operate from a very short runway, an area unsuited to conventional aircraft, which gives these aircraft certain tactical and strategic advantages that other aircraft do not have. This unique operation, however, is not amenable to conventional performance analysis. This is especially true of the engine downwash and the associated flow field along the ground.

Several problems are encountered during the normal operation of V/STOL aircraft. Since the discharge air from the engines is directed downward during take-off, hover, and landing, some means must be devised to protect the landing area from the downwash blast. Potential operational problems caused by this downwash include erosion of the landing surface, wind and debris hazards to nearby personnel and equipment, and possible damage to the aircraft itself. With jet aircraft, there is also a problem of hot gas reingestion under certain conditions.

In order to analyze any of these problems, an accurate knowledge of the downwash flow field, must be obtained. The most important section of the flow field, as far as landing-surface problems are concerned, is that portion that flows outward along the ground from the aircraft. It is this portion of the flow field that creates the serious ground erosion and recirculation problems.

Section II of this report describes general analytical methods of determining useful flow field parameters for various V/STOL aircraft. The most recent experimental data has been introduced, together with available theoretical methods of analysis. Both are combined to provide a nominal solution for the general flow field parameters based on the jet nozzle. The flow field is broken down into three regions and analytical equations are introduced for each. This section of the report is especially helpful to those interested in obtaining a complete study of the downwash flow field.

Section III of this report is devoted to a rapid method for estimating the groundwash parameters only at any desired point away from the aircraft. The equations are based on the theory presented in section II; assumptions have been made that allow solutions to groundwash parameters for both propeller and jet aircraft.

Section IV is a summary of the latest V/STOL research data pertinent to this problem. It consists of nozzle and rotor or propeller performance data, near-ground operational performance, general V/STOL engine evironment and aircraft performance data, and a summary of the specifications on the latest V/STOL aircraft.

SECTION II

OVERALL FLOW FIELD ANALYSIS

1. GENERAL FLOW FIELD DESCRIPTION

In general, the engine downwash is assumed to flow vertically downward until it encounters the ground, and then it spreads out radially over the ground. Since each type of V/STOL engine produces a different exit gas flow, analytical means may not be available to compute the downwash from each type of engine with any degree of accuracy. One analytical method has been established, however, to compute the downwash flow field of a jet nozzle accurately. It is these equations and certain modifications and assumptions that can be used to determine the flow fields of the remainder of the engines. Fortunately, the flow field along the ground, which is the most critical and important one for aircraft operation, lends itself to analytical solutions that can be applied to all types of V/STOL aircraft. Experimental data included in Section IV in graphical form can be compared with the analytical results contained in Section I.

2. FLOW FIELD AREAS OF ANALYSIS

Analytical studies of downwash phenomena in the past (see references) have shown that certain areas of the flow field lend themselves to quite accurate analysis, while others depend to a great extent on past experimental data and certain assumptions. The flow field has been divided into three regions, as shown in Figure 1 which are briefly described as follows:

a. Free Jet Region (Region I).

This region extends from the nozzle exit to an unlimited distance away from the exit. The nozzle discharge is not influenced by the ground in this region and, therefore, these equations are often used to determine free jet decay data. The static pressure within the nozzle downwash is assumed to be equal to the ambient pressure. As applied to V/STOL downwash data, which concerns itself with data within ten nozzle diameters (H/D = 10) above from the ground, this region terminates at the specific point above the ground where Region II begins.

b. Turning Region (Region II).

This region commences where Region I ends; it generally begins about one and one-half nozzle diameters (H/D = 1.5) above the ground and ends at a distance along the ground of about two nozzle diameters from the jet centerline. In this region, the direction of the air is turned from vertical to horizontal and the static pressure varies from a maximum at the jet centerline to ambient at the outer edge of the region.

c. Wall Jet Region (Region III).

The wall jet region extends from the end of Region II out to infinity (or to a point where the velocity is essentially zero). The flow is essentially parallel to the surface of the ground and moves radially outward in all directions from the jet centerline. The static pressure along the ground is equal to ambient.

These three regions which comprise the entire downwash flow field will now be discussed in detail. Equations will be presented and procedures for calculations will be listed.

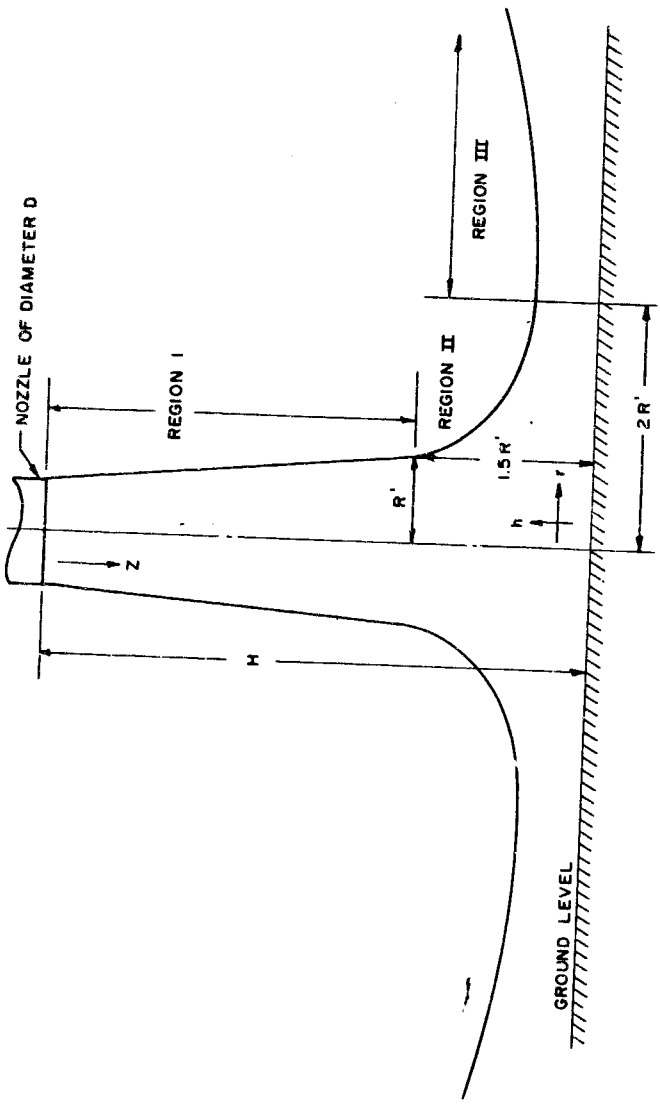

Figure 1. Schematic of Nozzle Downwash Flow

3. CALCULATION PROCEDURES

The calculations used to determine downwash parameters are based on a series of equations and graphs. The procedure is arranged so that the flow parameters can be calculated beginning at the nozzle (Region I) and extending down through Regions II and III. Thus, if only ground flow data is desired, for example, the preliminary equations of Region I or II can be easily eliminated from the analysis. This allows for a more rapid investigation of only those parameters that are pertinent to the problem. The equations and graphs have been presented in terms of ratios of velocity, pressure, temperature, and distance and are based on the nozzle exit conditions. Incompressible flow has been assumed in all areas ($P_T = P_o + 1/2 \rho V^2$). Additional detailed information on the theory and derivations of these equations can be found in References 1 through 7.

a. Free Jet Region (Region I)

The free jet region (Region I) is divided into three zones, as shown in Figure 2. The flow field in this region is similar to the flow from a nozzle or an orifice, and these flows have been examined previously by several investigators. Keuthe examined the turbulent mixing zones of a jet from a nozzle, subdivided the flow region into the three zones shown in Figure 2, and presented a solution for Zone I. Squire and Trouncer also examined the free jet region of a nozzle; the deriviation of their solutions for Zones I and II are presented in Reference 4. The work of these investigators was restriced to incompressible flow, however, and assumed a uniform velocity profile at the exit of the nozzle. This last assumption affects Zones I and II while the flow in Zone III will apply to any jet. The work of Keuthe appears to be the most complete. The expressions used in this report will be taken from the work of Squire and Trouncer, however, since their expressions are presented in a much simpler form, and the results agree quite well with Keuthe's results.

Zone I of the free jet region consists of a turbulent mixing shell surrounding a conical core whose velocity is equal to the exit velocity. At a point approximately 4.2 nozzle diameters downstream of the nozzle exit, the entire downwash becomes turbulent. Beyond this point, the centerline velocity begins to decrease, and the shape of the velocity profile approaches that of a parabola. Zone II extends from Z/D = 4.2 to Z/D=9 and the flow is entirely turbulent. The maximum velocity along the jet centerline at any distance away from the nozzle is well defined. The flow is essentially in transition and is developing the general flow characteristics of Zone III. Zone III begins at Z/D=9 and extends to the turning region. The maximum velocity in Zone III is inversely proportional to the distance Z + C, which is measured from the theoretical jet origin.

Equations are provided so that an outline of the jet downwash can be estimated. The procedures and equations for computing the parameters for the jet downwash are presented as follows.

(1) Zone I, Free Jet

The following equations can be used for calculating the parameters for the region between Z/D = 0 to Z/D = 4.2.

Core Area Equations

For $r \leq r_1$ $\qquad \frac{U}{U_m} = \frac{U_{max}}{U_m} = 1.0$

For $r_1 \leq r \leq r_o$

$$\frac{r_o}{R} = 1 + .03335\ Z/D \qquad (1)$$

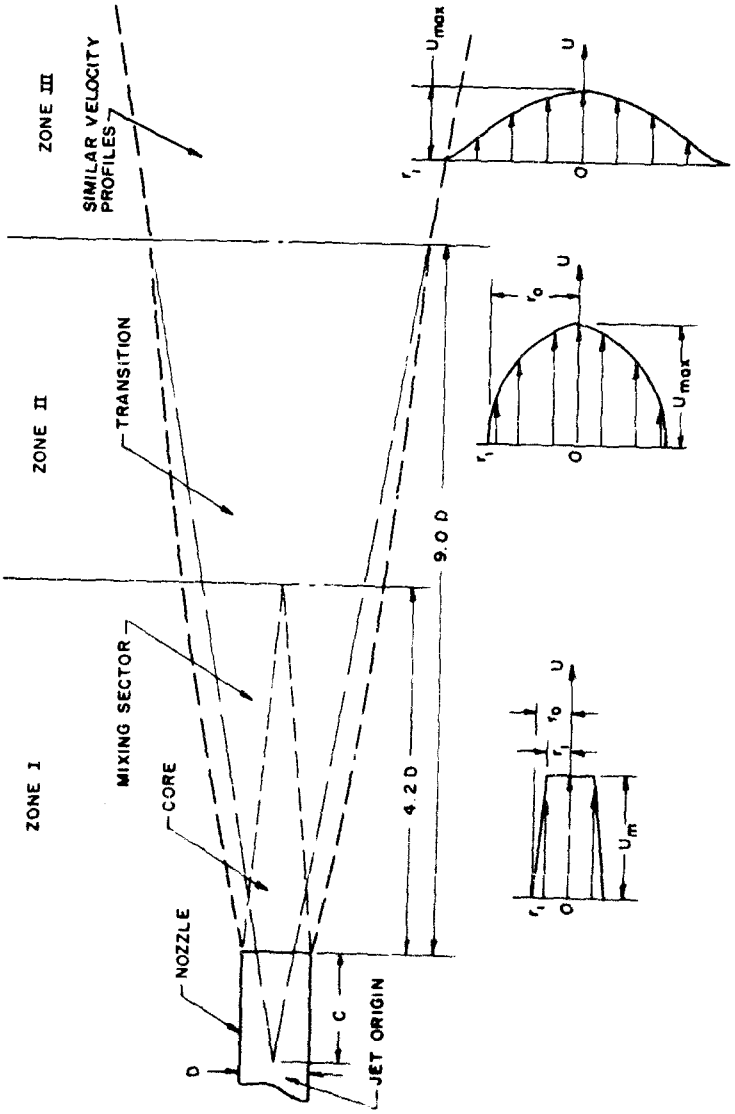

Figure 2. Axisymmetric Free Jet from a Circular Nozzle

Turbulent Area Equations

$$\frac{r_1}{R} = 1 - 0.238\ Z/D \tag{2}$$

$$\frac{U}{U_m} = \frac{1}{2}\left(1 - \cos\pi\left[\frac{\frac{r_o}{R} - \frac{r}{R}}{\frac{r_o}{R} - \frac{r_1}{R}}\right]\right) \tag{3}$$

(2) Zone II, Free Jet

The following equations can be used for calculating the parameters for the region between Z/D = 4.2 to Z/D = 9.0.

$$\frac{U_{max}}{U_m}, \quad \text{determine from Figure 3}$$

$$\frac{r_o}{R} = 1.2 + 0.2865\ Z/D \tag{4}$$

$$\frac{U}{U_{max}} = \frac{1}{2}\left(1 + \cos\pi\left[\frac{\frac{r}{R}}{\frac{r_o}{R}}\right]\right) \tag{5}$$

(3) Zone III, Free Jet

The following equations can be used for calculating the parameters for the region between Z/D = 9.0 and the turning region, Region II.

$$\frac{U_{max}}{U_m} = 6.57 / (Z/D + C/D) \tag{6}$$

$$\frac{U}{U_{max}} = \left[1 + 57.56\left(\frac{r}{Z + C}\right)^2\right]^{-2} \tag{7}$$

C/D = 1.44 (for a nozzle with a uniform exit velocity)

This completes the equations for Region I.

There is a discontinuity of the velocity profiles between Zones II and III which is caused by the different flow assumptions used in each zone. The Zone III equations, which were taken from Schlichting, provide values that are considerably more accurate than those for Zone II. In general, the downwash from any hovering vehicle will develop Zone III flow characteristics at a Z/D = 9. Unfortunately, in most of the work considered in this report, the turning region begins at Z/D ratios much lower than 9.0. In this case, these equations may not be very useful.

b. Turning Region (Region II)

The turning region has been defined as that portion of the downwash where the general direction of flow changes from vertical to horizontal along the ground. The flow may enter Region II from any of the zones of Region I; for this analysis, the turning region has been defined as having an initial radius of R' at a height of 1.5R' above the ground (see Figure 1) and is assumed to end at a distance of 2 R' along the ground from the jet centerline. The profiles

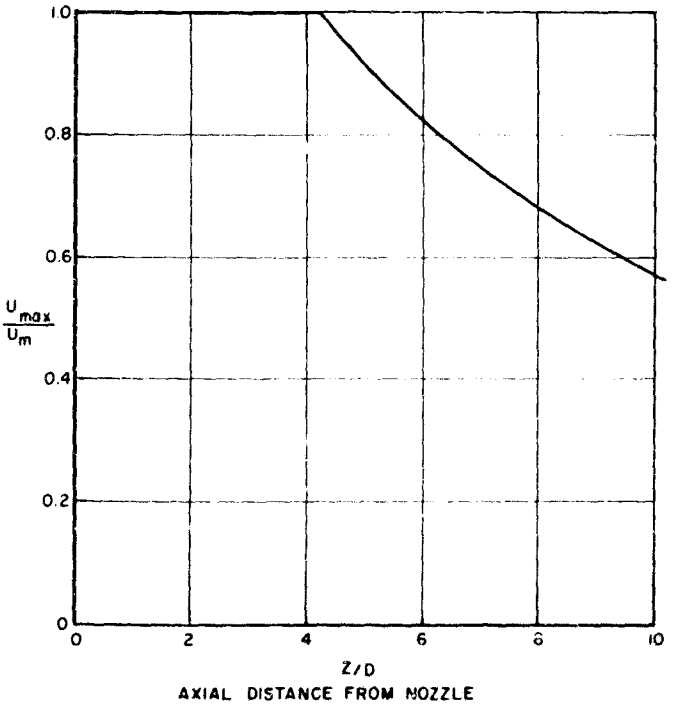

Figure 3. Center Line Velocity of Zones I and II of Region I

of the zones in Region I have different boundary equations: therefore, different expressions must be used to determine the values of R'. The following equations define R' for each of the ranges in which the turning region might start:

Equation	Useful Range
$R'/R = 0.0461\ H/D + 0.9654$	$0 \leq H/D \leq 5.1$
$R'/R = 0.1310\ H/D + 0.5420$	$5.1 \leq H/D \leq 10.4$
$R'/R = 0.1505\ H/D + 0.2167$	$10.4 \leq H/D \leq \infty$

The maximum velocity along the ground will occur at the exit of the turning region, at the distance $r = 2R'$ from the jet centerline. This location of maximum ground velocity is the point where ground erosion is expected to start. The magnitude of this velocity (V_g) is assumed to be equal to the maximum vertical velocity of Region I, at the distance $Z = H+2R'$. The appropriate equation for Region I or Figure 3 may be used to determine this value. Equations that can be used to determine the height of the maximum velocity along the ground are included with the equations for the wall jet region.

A review of the literature on flow fields yielded very little information pertaining to the turning region. No practical theories could be found to describe this region with any degree of accuracy. The expressions and assumptions defining the flow field presented here contain most of the information found. These assumptions include:

(1) The flow is isentropic;
(2) Incompressible flow equations are applicable;
(3) The nozzle discharge velocity profile is uniform;
(4) The flow is perpendicular to a large flat plate;
(5) The nozzle is located at least 3 radii away from the flat plate.

Most of the investigators conducted their research using assumptions similar to these.

A more detailed study of the turning region is presented in Reference 6. A synopsis of that work is presented in the remainder of this subsection for the convenience of those readers who are interested. The theory is shown graphically in Figures 4, 5, and 6.

The flow near the intersection of the nozzle centerline and the ground is described as follows:

$$V_x = ax \tag{8}$$

$$V_y = 2ay \tag{9}$$

$$\psi = ax^2 y \tag{10}$$

where a = constant
x = horizontal distance parallel to the ground
y = vertical distance
V_x = horizontal component of velocity
V_y = vertical component of velocity
ψ = stream function, constant along any streamline.

The constants are evaluated as follows: The line for constant velocity potential that passes through the point where the ground and the jet centerline meet will be straight with a slope of $1/\sqrt{2}$. The velocity will vary linearly along this line from zero at the origin to U_m on the

free stream line. The coordinates of the free stream line and the velocity potential line may be found by means of the continuity equation. The nozzle exit flow may then be set equal to the flow across the velocity potential line. The velocity (v) at any point along the velocity potential line may be given by:

$$v = U_m \, (x / x_e)$$

where x_e equals the radius to the edge of the fluid flow. Making use of the continuity equation gives:

$$\pi R^2 U_m = \int_0^{x_e} v \, dA = 2\pi \sqrt{3/2} \int_0^{x_e} U_m \, (x/x_e) \, x \, dx \qquad (11)$$

Solving Equation 11 yields:

$$x_e = 1.1067 \; R = r$$

$$y_e = 0.7825 \; R = h$$

Then

$$V_x = (U_m \; a'/R) \, r \qquad (12)$$

$$V_y = 2 \, (U_m \; a'/R) \, h \qquad (13)$$

At the intersection point,

$$U_m^2 = V_x^2 + V_y^2$$

Substituting the coordinates in the above equation and letting U_m equal unity, we obtain $a' = 0.5217$.

The velocity along the ground ($y = 0$) and along the jet center line ($x = 0$) may be found by using Equations 12 and 13. Since the velocity (v) cannot exceed U_m and P_T is a constant, substituting into the incompressible flow equation for the static pressure along the ground yields.

$$P = P_T - \frac{1}{2} \rho \, (0.5217 \, U_m \, r/R)^2$$

Dividing by P_T gives:

$$P/P_T = 1 - (0.5217 \, r/R)^2 \; (\rho U_m^2 / 2 P_T)$$

Since P_T = total pressure = $1/2 \rho U_m^2$

$$P / P_T = 1 - 0.2722 \, (r/R)^2 \qquad (14)$$

The jet center line static pressure is shown in Figure 4. The agreement between the experimental data and theory is accurate to a height of only about $h/D = 0.4$. The static pressure along the ground is shown in Figure 5. The agreement here extends out to a radial distance of about one nozzle diameter. Using the incompressible flow equation to determine the appropriate velocities, we obtain Figure 6. Again the agreement between experiment and theory is quite good. It is well to note here that there is almost complete recovery of the nozzle exit velocity, even for nozzle heights of 4.0.

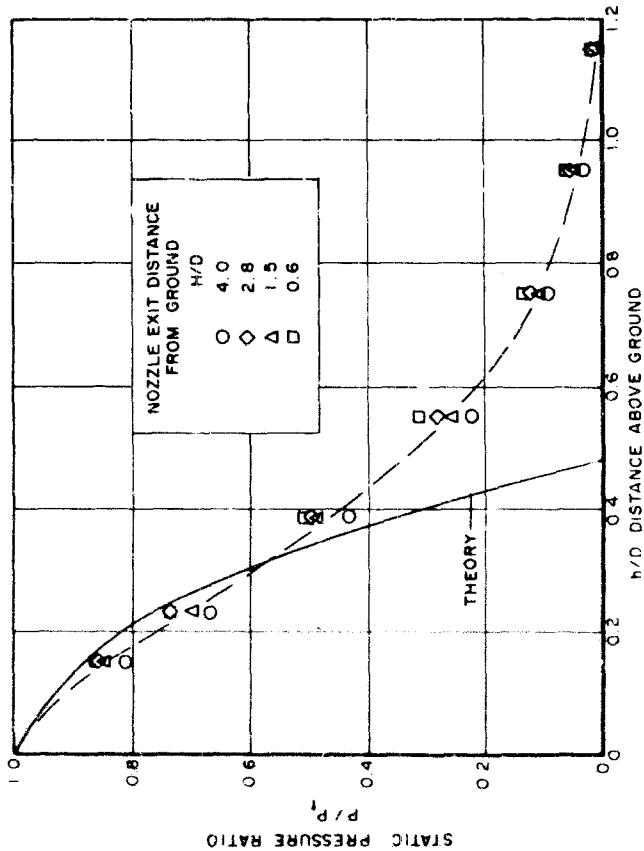

Figure 4. Nozzle Center Line Static Pressure Ratio in the Turning Region

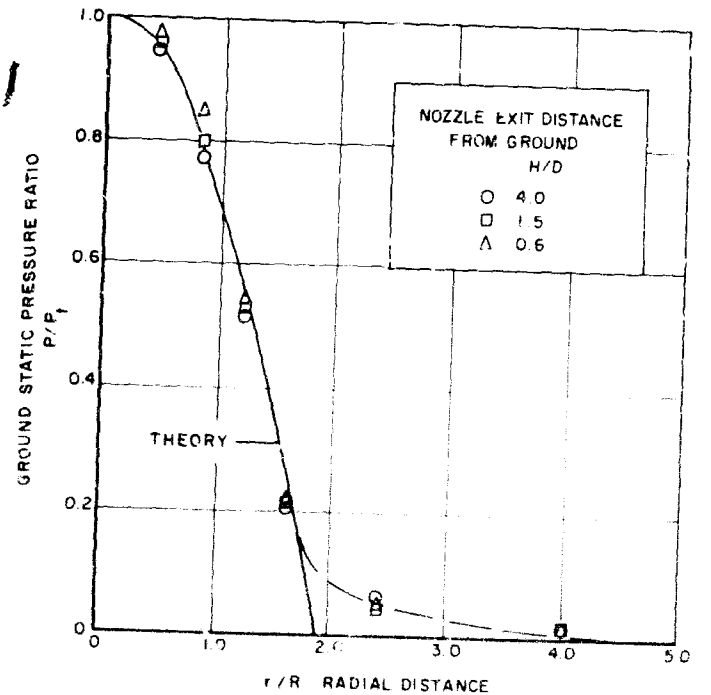

Figure 5. Ground Static Pressure Ratio in Region II

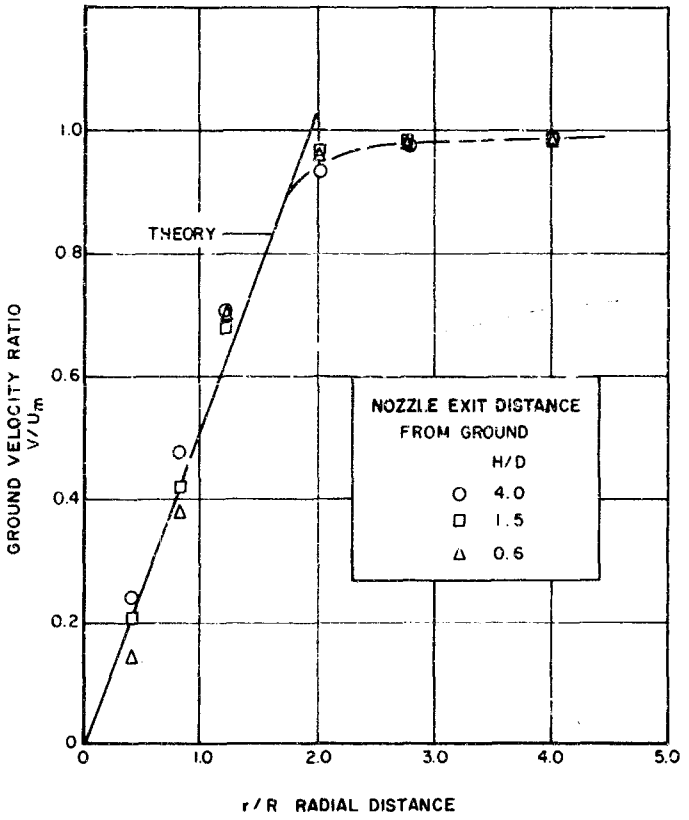

Figure 6. Ground Velocity Ratio in Region II

Equation 14 may be generalized by introducing the previously developed term R', which is the radius of the free jet profile at the beginning of the turning region and at a height of 1.5 R' above the ground.

$$P / P_T = 1 - 0.2722 \, (r/R')^2 \qquad (15)$$

This equation should be used only over that interval where theory and experimental data agree.

As previously stated, the attempts to develop any general expressions for the flow throughout the turning region have been unsuccessful. The previous assumptions may be quite naive in some applications, but they are useful in view of the correlation of Figures 4, 5, and 6 with experimental data. It still appears, however, that the best description can be obtained from actual test data under realistic conditions.

c. Wall Jet Region (Region III)

The flow in the wall jet region moves radially along the ground away from the jet center line. This region is assumed to begin at r = 2R' and to continue out to r = ∞, (infinity) or to the point where the ground velocity becomes zero. The region is broken down into two zones as shown in Figure 7. Zone A starts at r = 2R' and continues to r = 5 R'. Special analysis must be conducted here, since the flow is in transition from the turning region and develops the general characteristics of Zone B. Zone B begins at r = 5R' and continues out to infinity.

The only useful information to describe Zone A was obtained from experimental data. The curve in Figure 7 describing the decrease in maximum velocity was taken from Reference 11. In Zone B the rate of decay of the velocity and a velocity profile have been established by Glauret and by Poreh and Cermack. The work of Glauret will be used here since it appears to give the best results. Only the basic equations will be presented here; a more detailed investigation can be obtained from References 5 and 12.

Figure 7 shows the decrease in maximum velocity throughout Zone A. The data is presented as a function of velocity entering the turning region; this velocity was determined to be that of the free jet region at a distance Z = H + 2R' from the exit of the nozzle. The height of maximum velocity in the ground slipstream in Zone A will be estimated from information obtained in Zone B.

The equations describing the flow in Zone B of Region III are presented below. They are similar to the equations in Region I, and provide a method of obtaining the rate of decay of the ground velocity and of determining the velocity profile at any station along the ground (see Figure 8). The procedures for calculating these parameters are as follows:

For the beginning of Zone B at r = 5R',

(1) Obtain V_{max} from Figure 7 at r = 5R';
(2) From standard air tables determine the kinematic viscosity of the air;
(3) Calculate δ from the following equation:

$$\delta = \frac{0.134 \, R^2}{R' \left(\frac{V_{max}}{U_m}\right)^2} \qquad (16)$$

(4) Evaluate the term $\frac{V_{max}\delta}{\nu}$ and obtain the wall jet reynolds number from figure 9. (For simplicity, the reynolds number may be assumed constant throughout Zone B.)

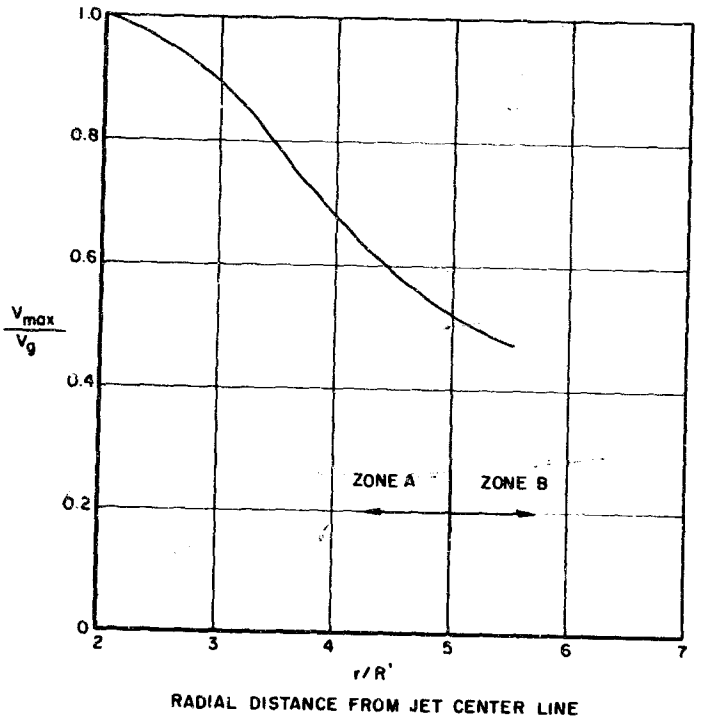

Figure 7. Maximum Velocity of Flow in the Wall Jet Region

(5) Calculate δ_m/δ from the following equation:

$$\delta_m/\delta = 1.3 / 1.3 + RN^{0.191} \quad (17)$$

(6) Determine the values of a, b, and α From figure 10.
(7) Determine the maximum velocity, V_{max}, and the height, δ, at any distance, r, in Zone B by using the following equations:

$$V_{max} = (V_{max})_{5R'} \ (5R'/r)^{\alpha} \quad (18)$$

$$\delta = (\delta)_{5R'} \ (r/5R')^{b} \quad (19)$$

(8) Evaluate from Figure 11, the actual velocity profile, using the results of the above equations.
(9) Assume for Zone A, that the height of the maximum velocity varies linearly from a value of zero at the jet center line to the value δ_m at $r=5R'$.

No equations have been developed to describe the flow in Zone A of Region III since this flow is in transition. The assumption made in Step 9 appears reasonable, however, from an analysis of pressures and velocities in the turning region and the established equations of Zone B in Region III.

4. GENERAL CONSIDERATIONS

The accuracy of the results of these equations is limited by the assumptions used in establishing the calculating procedures. The usefulness of the equations will depend on how well the assumptions fulfill the requirements of the particular application.

The equations in Region I are accurate to about 5% for nozzles of uniform exit velocity. The equations for Zone 3 of Region I are the most accurate of all those presented, but they may not be particularly useful for near-ground V/STOL calculations. The value of "C" will vary for each type of propulsion system. Values between one and two will cover most nozzles, the value for rotors or propellers, however, may be negative. Very little work has been done in this area so far as determining these coefficients for various propulsion systems.

Equations and data for evaluating the turning region are nonexistent. Most of the values here are predicted from the data of Regions I and III and are based mostly on experimental data. Ground pressure data from experimental methods also help in estimating this data; however, information on the amount of turbulence, the turning losses, and the exact physical extent of the region are nonexistent.

Determining values for Zone A of Region III is also highly dependent on experimental information. Theory for Zone B is reasonably well established; however, values from some of the assumptions made in Zone A are carried over to Zone B, along with any inherent error.

5. CONCLUSIONS AND RECOMMENDATIONS

A useful system has been presented to calculate the major parameters of V/STOL engine downwash. The effectiveness and accuracy of these equations are based on the propulsion system used, the accuracy of the assumptions presented, and the compatibility of the experimental data with the desired information.

If truly accurate downwash information is required, then the following areas will require specific investigation:

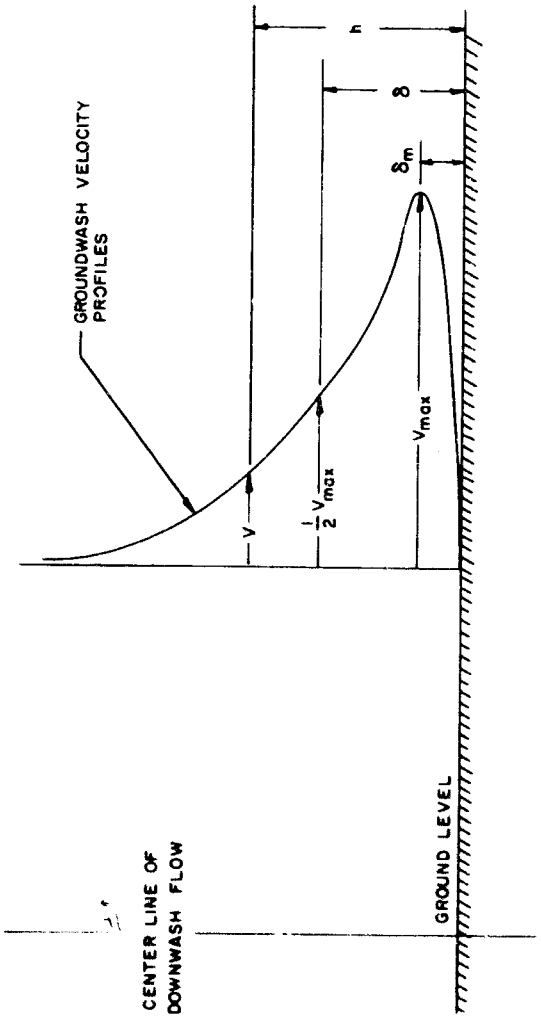

Figure 8. Nomenclature for Zone B of Region III

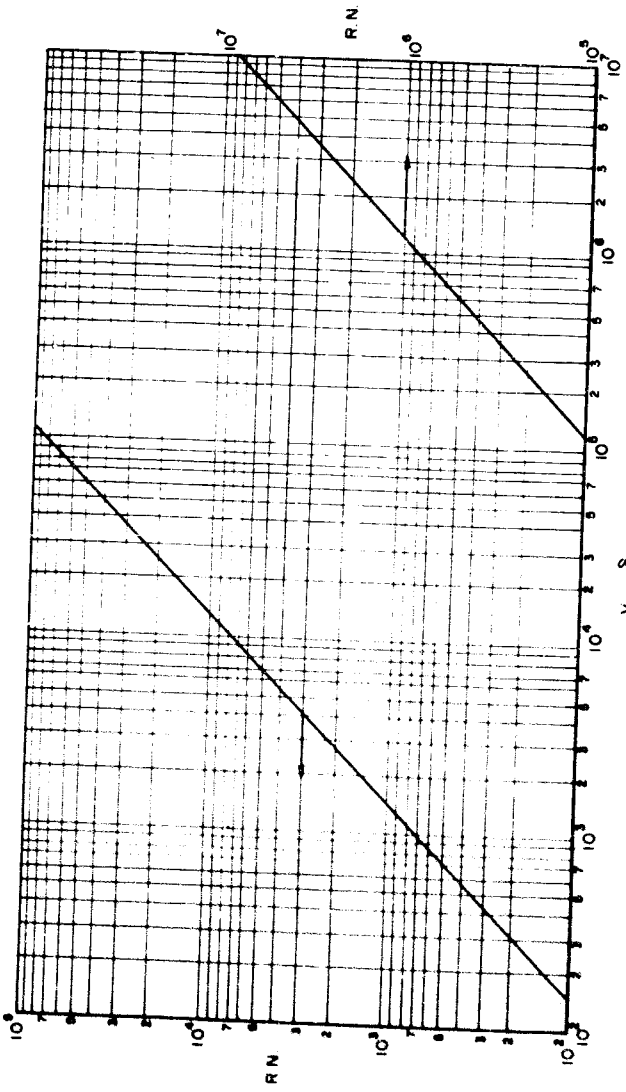

Figure 9. Reynolds Number for Region III

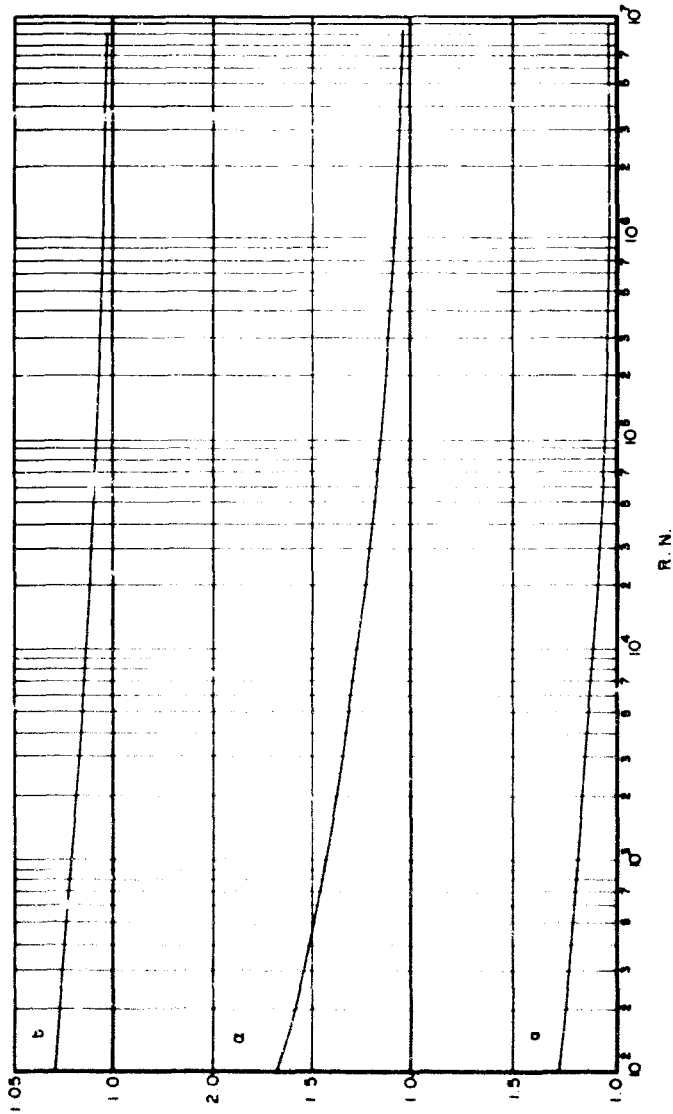

Figure 10. Parameters a, b, and σ Versus Reynolds Number

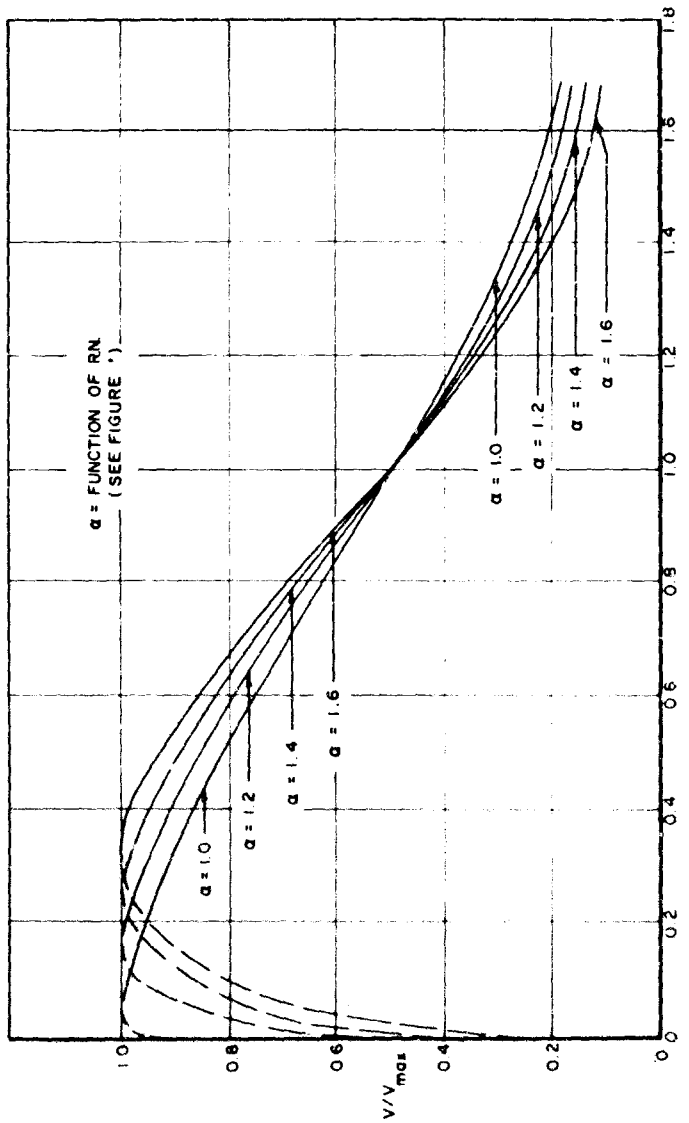

Figure 11. Velocity Profiles for Zone B of the Wall Jet Region

a. The effect of nonuniform exit velocity profiles on the engine downwash.
b. Mixing effects caused by gases of varying densities exiting into air.
c. The turning region (including overall turning losses), actual physical extent of the region, and an accurate analysis of the location and the change in maximum velocity within the region.
d. Zone A of Region III where the ground flow is in transition.

SECTION III

GROUNDWASH ANALYSIS

1. GENERAL FLOW FIELD DESCRIPTION

In many instances, Regions I and II of the downwash flow field are of little interest to the reader. They take place very near the aircraft. Depending on the aircraft configuration, the flow field near the aircraft may be disrupted to the point where any desired calculations would be in error. Of great importance to many engineers, however, is the extent of the groundwash at greater distances from the aircraft. This is important in regard to determing the required landing area and providing protection for personnel and equipment.

It has been shown in Section II that the flow in Zone B of the wall jet region lends itself to an analytical solution of the groundwash parameters The solutions presented here are based on these equations. This section will provide a means of estimating the extent of the groundwash for various V/STOL aircraft. This estimation will be based on the type of aircraft and on the number of its engines. The remaining assumptions are contained in the following analysis.

a. Jet Aircraft Analysis

In determining the ground pressure or velocity decay at any radial point away from the aircraft, the following assumptions are made.

(1) The flowfield at the beginning of Region I has an area equivalent to the sum of the exit areas of the individual lift engines of the aircraft.
(2) The exit velocity is uniform over this equivalent area and impinges normally on a relatively flat surface.
(3) The centerline of the equivalent nozzle area coincides with the centroid of the areas of the individual nozzles.

The solutions presented here provide for a means of bypassing the initial downwash equations of Section II and allow for an immediate solution of the groundwash at any desired distance from the aircraft. Equation 18 Section II defines the maximum velocity along the ground (V_{max}) as a function of the distance (r) from the aircraft:

$$V_{max} = (V_{max})_{5R'} (5R'/r)^a \tag{20}$$

Dividing by U_m and for distances $r > 5R'$, Equation 20 becomes

$$\frac{V_{max}}{U_m} = \left(\frac{V_{max}}{V_g}\right)_{5R'} \left(\frac{V_g}{U_m}\right) \left(\frac{2.5R'D_e}{rR}\right)^a \tag{21}$$

At entering Zone B of Region III, $V_{max}=0.521\ V_g$. Then

$$\frac{V_{max}}{U_m} = 0.521 \frac{V_g}{U_m} \left(\frac{2.5R'}{R}\right)^a \left(\frac{D_e}{r}\right)^a \tag{22}$$

where V_g/U_m is determined from Figure 12 at the value where Z/D=H/D, R'/R and R'/R is defined in Equations of Section II b with the appropriate H/D value.

The exponent, a, in the above equations is a function of Reynolds Number as shown in Figure 10. For simplicity, an average value of 1.15 is assumed. Equation 22 then becomes:

$$\frac{V_{max}}{U_m} = 1.493 \frac{V_g}{U_m} \left(\frac{R'}{R}\right)^{1.15} \left(\frac{D_e}{r}\right)^{1.15} \tag{23}$$

which may be written as

$$\frac{V_{max}}{U_m} = K \left(\frac{D_e}{r}\right)^{1.15} \tag{24}$$

and

$$K = 1.493 \frac{V_g}{U_m} \left(\frac{R'}{R}\right)^{1.15} \tag{25}$$

since D/r is not a function of R'/R or V_g/U_m.

Figure 13 has been plotted to determine at which H/D value the term K is a maximum. It can be seen that r/D for a particular V_{max}/U_m is a maximum at H/D = 3.914. This is the condition for maximum extent of the ground flow, and this value will be used to determine the final equations.

The groundwash diameter, D_{req}, as a function of either the velocity or the pressure at any desired point can be obtained from Equation 24

where

$$\frac{r}{D_e} = K^{\frac{1}{1.15}} \left(\frac{U_m}{V_{max}}\right)^{\frac{1}{1.15}}$$

$$r = \frac{D_{req}}{2}$$

Then

$$\frac{D_{req}}{2\,D_e} = (1.75)^{\frac{1}{1.15}} \left(\frac{U_m}{V_{max}}\right)^{\frac{1}{1.15}}$$

or

$$D_{req} = 3.256\,(D_e) \left(\frac{U_m}{V_{max}}\right)^{\frac{1}{1.15}} \tag{26}$$

Also

$$D_{req} = 3.256\,(D_e) \left(\frac{q_n}{q_{max}}\right)^{\frac{1}{2.3}} \tag{27}$$

For nozzles, in-wing fans, or ducted fans,

$$q_n = T/A_e \tag{28}$$

It should be noted that the diameter D_e in Equations 26 and 27 represents the equivalent diameter of all the nozzles of the aircraft as discussed at the beginning of this section. If N engines of equal size are used, then

$$D_e = \sqrt{N}\,(D) \tag{29}$$

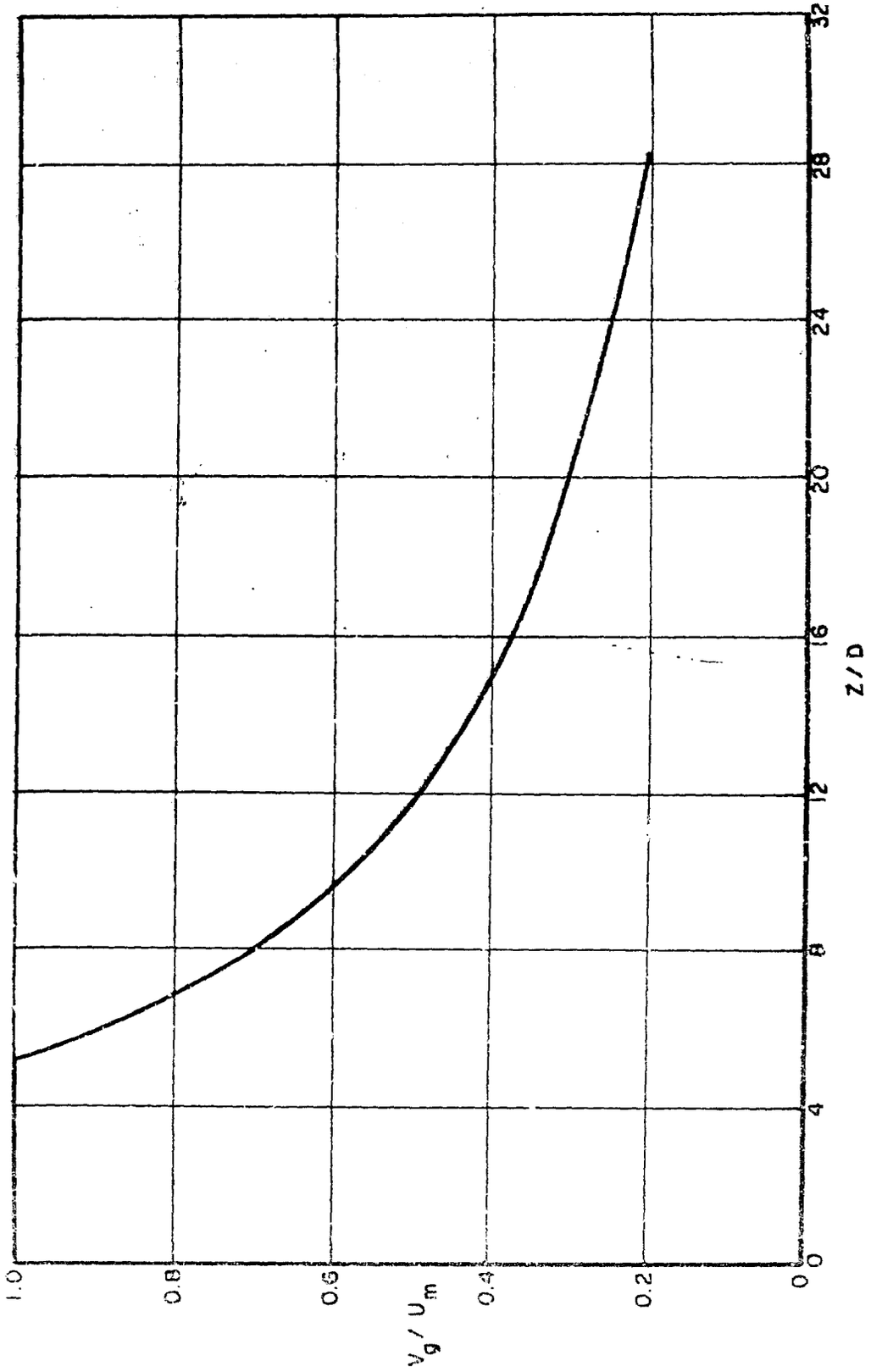

Figure 12. Maximum Ground Velocity at Various Distances from Jet Exit

Equations 26 and 27 then define the maximum velocities and pressures at any desired distance from the aircraft. For example, assume a single jet engine 1 foot in diameter has an exit gas velocity of 1500 ft/sec. At what distance from the aircraft will the velocity be 50 ft/sec.?

From Equation 26,

$$D_{req} = 3.256(1)\,(1500/50)^{\frac{1}{1.15}} = 63 \text{ feet}$$

The distance from the engine centerline would be approximately 31.5 feet.

b. Propeller-Rotor Aircraft Analysis

A review of the available literature yielded very little information on the dynamic pressure decay of the downwash from a rotor or propeller. Most of the information presented here is based on References 11 and 14.

Equations are needed to determine at what height the rotor or propeller will produce the maximum ground dynamic pressure. The work is similar to that performed in Section II. From Equation 25:

$$K = 1.493\,\frac{V_g}{U_m}\left(\frac{R'}{R}\right)^{1.15}$$

V_g/U_m can be obtained from Figure 14 at $Z/D = H/D + R'/R$, where $R'/R = 0.0461\,H/D + 0.9654$, assuming a maximum value of $0<H/D<5.1$. Again, plotting K vs. H/D shows that V_g/U_m for a particular r/D is a maximum at H/D = 0.4. This is shown in Figure 15. All calculations will now be based on this value. For H/D = 0.4, R'/R = 0.984, and from Figure 7 V_{max}/V_g may be plotted against r/D. Since $Z/D = H/D + R'/R = H/D + 2R'/D = 0.4 + 0.984 = 1.384$, from Figure 14 Z/D = 1.384 and $V_g/U_m = U_{max}/U_m = 1.006$. Using these values the variation of V_{max}/U_m may be obtained with r/D_e. The corresponding pressures q_{max}/q_e with r/D_e is plotted in Figure 16 where r equals the required radius = $D_{req}/2$ and D_e equals the equivalent rotor or propeller diameter. Also $D = 0.707\,D_{prop}$ and $D_e = 0.707\sqrt{N}\,D_{prop}$.

Figure 16 allows for the solution of groundwash problems involving propeller or rotor aircraft.

For Example, assume a helicopter has a 60-foot diameter rotor with a disk loading of 7psf. At what distance from the helicopter will the dynamic pressure of the surface downwash decay to 3 psf?

$$D_e = 0.707\sqrt{N}\quad D_{prop} = 0.707(60) = 42.5 \text{ feet}$$

and

$$\frac{q_{max}}{q_e} = 3/7 = 0.429.$$

From Figure 15 $r/D_e = 2.03$

Then

$$r = 2.03\,(42.5) = 86.3 \text{ feet}.$$

The required distance, therefore, would be 86.3 feet from the rotor center line.

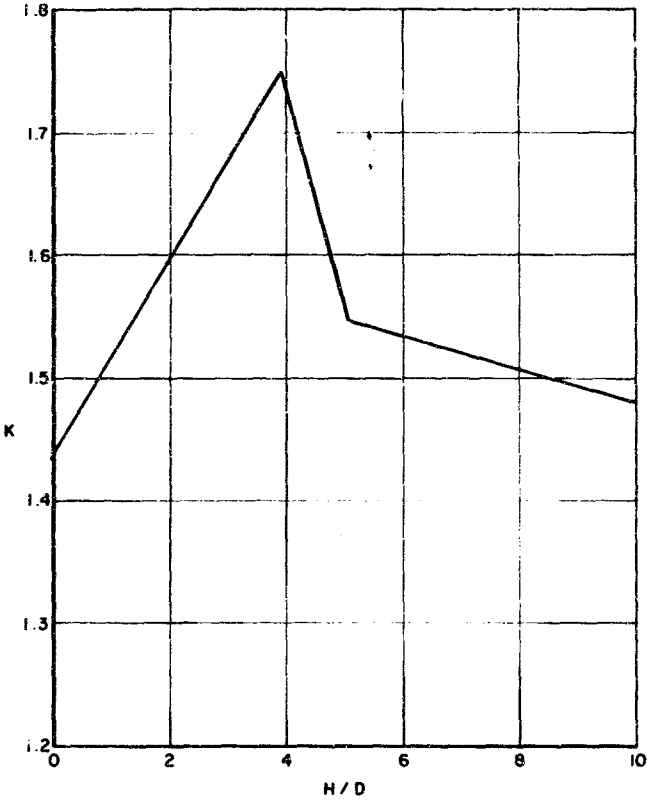

Figure 13. Variation in K From Equation 25 for Various Nozzle Exit Heights

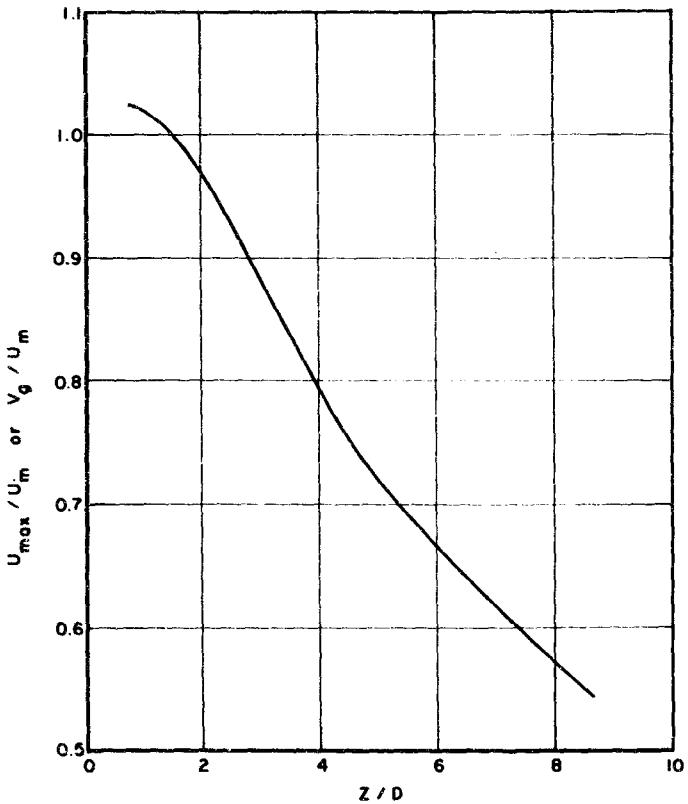

Figure 14. Maximum Ground Velocity at Various Distances From the Propeller Exit

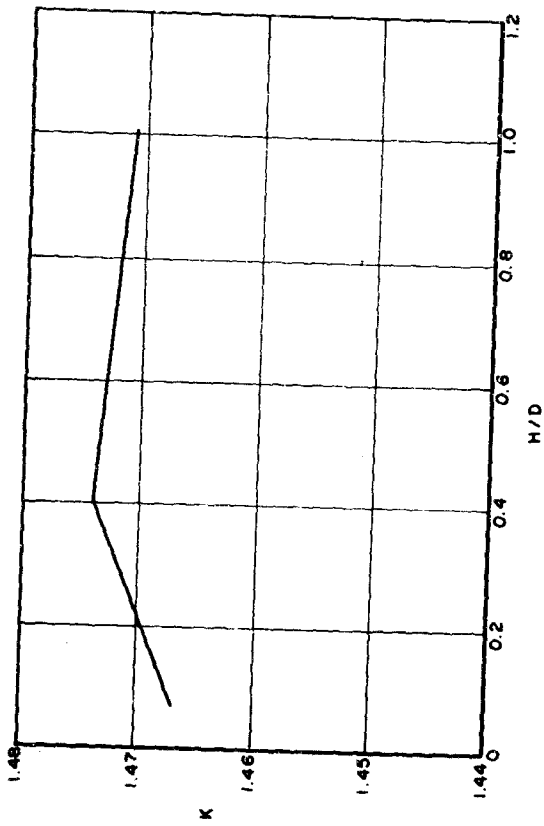

Figure 15. Variation in K of Equation 25 for Various Propeller Exit Heights

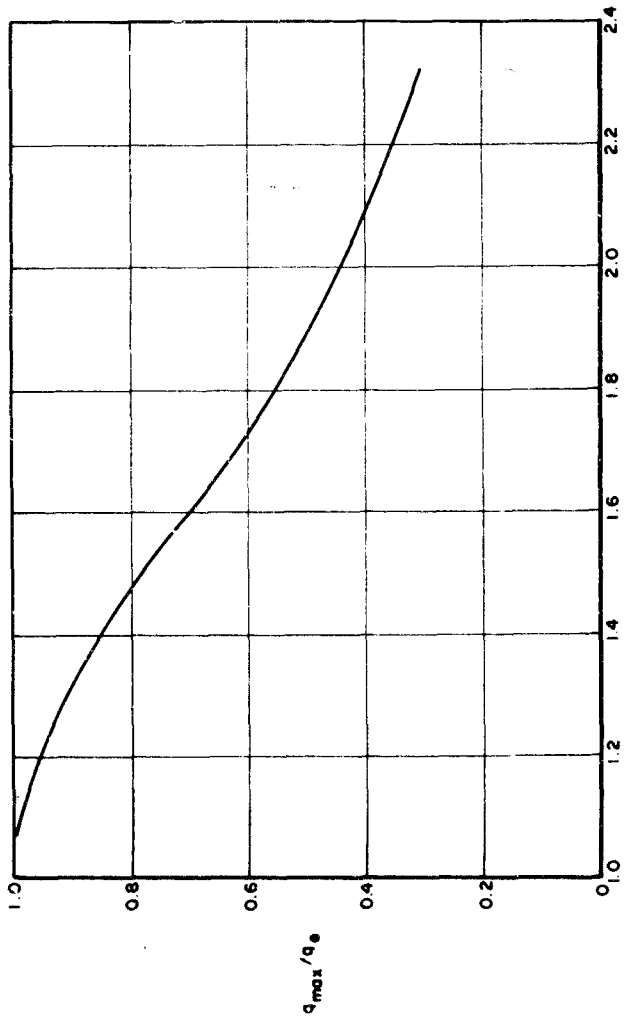

Figure 16. Ground Dynamic Pressure Decay for Propeller or Rotor at H/D = 0.4

2. GENERAL CONSIDERATIONS

In order to verify the analytical approaches given above, a research of available downwash data was conducted in both areas. References 15 and 16 provided the only useful data found for a single jet impinging on a flat surface. Figure 17 shows the correlation between this data and the above theory. The agreement appears good.

There is virtually no data for flow fields created by more than one jet. Reference 17 contains flow field data for three types of propeller VTOL aircraft, but quantative data is not available because height to diameter ratios are not given for the listed data.

To obtain multijet flow data, LTV Vought Aeronautics conducted tests with the XC-142A aircraft. Final data is still being compiled, but preliminary analysis shows adequate correlation in view of the limited amount of data.

3. CONCLUSIONS AND RECOMMENDATIONS

The equations and data presented in this section allow for a reasonably accurate calculation of the ground downwash parameters. The error is estimated to be less than 20% in all cases and as little as 5% in the work involving the jet nozzle.

Other items that have not been considered are the configuration of the aircraft itself, the location of the wing and its planform, the closeness of the engine exits to the ground, and the relative flatness of the ground itself. All these factors have a great influence on the flow along the ground. Another important physical parameter that is often ignored is the ambient wind condition. This parameter would appear to have a great effect on the extent of the surface flow relative to the other factors.

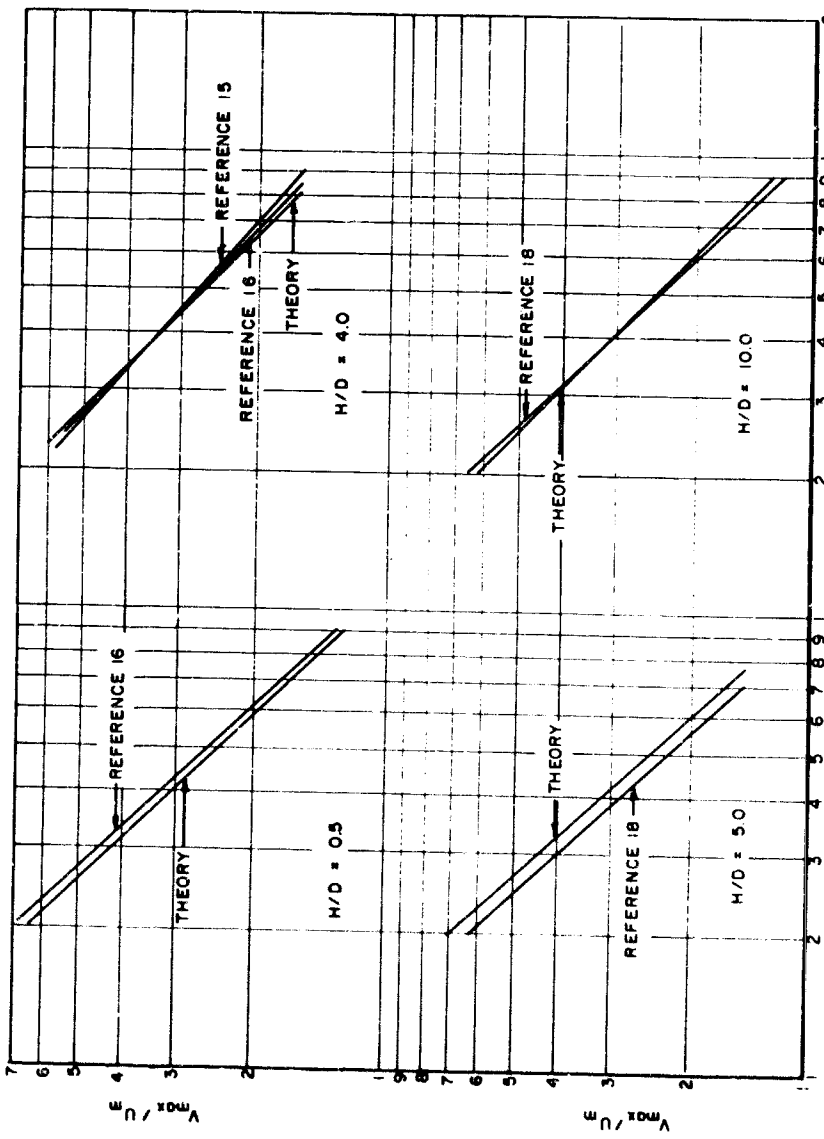

Figure 17. Correlation of Theoretical and Experimental Data of Ground Dynamic Pressure Decay

SECTION IV

SUMMARY OF V/STOL EXPERIMENTAL DATA

This section contains the latest research data on downwash in the area of V/STOL experimentation. Most of the data presented here has been obtained experimentally, but theoretical curves are furnished for purposes of comparison. The purpose of this section is to present a general comprehensive tabulation of the latest experimental data on V/STOL propulsion systems and aircraft including the following:

a. Jet nozzle performance data
b. Rotor and propeller performance data
c. Near-ground operational performance
d. General V/STOL engine environment and aircraft performance data
e. Summary of V/STOL aircraft specifications

Although this discussion is not intended to interpret in detail all the graphical information presented here, those figures where misunderstandings might occur will be briefly discussed to clarify the intent.

1. JET NOZZLE PERFORMANCE DATA

Figures 18 through 26 present information based primarily on a nozzle pressure ratio of 2.0. This pressure closely parallels the operational pressure of a nozzle on a jet engine at military power. Some of the curves also include nozzle operation at 1200 °F, which, combined with the pressure ratio data, allows for very accurate estimations of actual jet nozzle performance. The difference between operating with an ambient temperature gas and the 1200 °F gas as applied to the downwash decay parameter is shown in Figure 19. The difference in values between the two curves shows the relative difference in mixing of the two exit gases when discharged into ambient air.

Figure 20 shows the reduction in exit gas temperature with distance from the nozzle. The effect of nozzle operation at 5 nozzle diameters above the ground is shown in Figure 22. The values for pressure and temperature with ground effect were slightly less than those for free air. The exact reason for this is not completely understood since no accurate knowledge of the airflow in this region is available.

Figure 23 presents the findings of three different investigators in the study of maximum surface velocity. A wide variation appears to exist in the curves of this figure. This variation exists because maximum recovery of the nozzle velocity is a function of H/D, and the curves are based on different values of H/D. The curve of Reference 11 is based on an ambient airflow at an H/D $\approx$ 1.0, and that of Reference 29 is based on a pressure ratio of 2.0, a gas temperature of 1200 °F, and an H/D of approximately 5.0. Correcting these curves for one pressure, temperature, and height ratio would have resulted in very close agreement of this data.

The effect of nozzle pressure ratio is shown in Figure 24. The slight decrease in downwash decay at the higher pressure ratios is attributed to the effects of compressibility, which start at a pressure ratio of about 2.0. At greater distances from the engine, the compressibility becomes almost negligible.

Pressure and temperature profiles over the ground surface are shown in Figures 25 and 26. The data is plotted for a nozzle height of 5.0 diameters, which is typical of operational nozzle heights for current design VTOL aircraft. Data is plotted for five different radial stations away from the nozzle center line.

An effort has been made to present this data with parameters that could provide a direct comparison of the data of each reference. Different instrumentation techniques were used, however, and there were generally different test objectives, so this is seldom possible. The technique used in Reference 28, where the pressures and temperatures are presented as differentials, appears to provide the best test data. As previously mentioned, it also closely simulates actual jet nozzle operation.

2. ROTOR AND PROPELLER PERFORMANCE DATA

The curves presented in Figures 27 through 32 are based on data obtained in experiments using a two-foot diameter rotor. Most of the information was obtained from Reference 23. With certain reservations, the information presented here could also be applied to propeller systems, particularly to the near-ground performance charts.

Figure 27 shows the difference between two theoretical assumptions of disc loadings for the fully developed wake and the values measured at the rotor plane and 1.2 radii below the rotor plane. Variations in the number of blades, the collective pitch, and other parameters would produce certain quantitative differences in load distribution but the general configuration of the curve would be the same.

The difference in slipstream profiles of a ducted fan and a propeller are shown in Figure 28. As expected, the exit profile for the ducted fan is much more uniform than that for the open propeller. This uniformity is the result of the ducting around the fan, which prevents the normal contraction of the slipstream. The decay rates are almost identical at distances beyond two exit diameters. The open propeller or rotor realizes a significant increase in lift at low height-to-diameter values. Rotors may operate at H/D ratios of 0.25 when taking off, so this induced lift is very beneficial. The ducted fan obtains some induced lift, but the amount is highly dependent on blade angle (See Figure 36).

Figures 29 and 30 show the velocity distribution and static pressure contours for a rotor at near-ground operation and for one operating out of ground effect. The velocity contours are different because in near-ground operation the wake cannot develop fully before the downwash is turned along the ground. Relatively high upward velocities are evident at the rotor center line, and negative static pressures are experienced at the blade tip due to the rotor tip vortices. The effective stagnation point in the downwash is located at a distance of about 0.8 radius. The pressure drops off rapidly beyond this point with the rapid acceleration of the downwash along the ground. Inboard of this point there is a relatively high but constant pressure distribution as a result of the two converging downwashes under the rotor center line.

Figure 31 shows that the ground static pressure increases as the rotor height decreases, but only to a certain ratio. At a rotor height of about 0.5 radius, a sharp drop in the ground pressure appears, which is believed to be caused by a high velocity vortex escaping at the rotor center line. Although it is not completely understood, it is probably a result of the conservation of angular momentum of the air flowing radially inward along the ground.

The ground velocity profiles in Figure 32 show some peculiar characteristics. At stations 2.4 and 3.4 radii from the center line, the maximum velocity increases rather than decreases with rotor height up to a height of 5 radii. This characteristic is assumed to be the result of the difference in wake profiles observed at station 1.5. A narrower high-speed wake tends to dissipate more quickly than a wider moderate-velocity wake. The larger static pressure potential at station 1.5 also may tend to accelerate the wakes of the higher rotor positions.

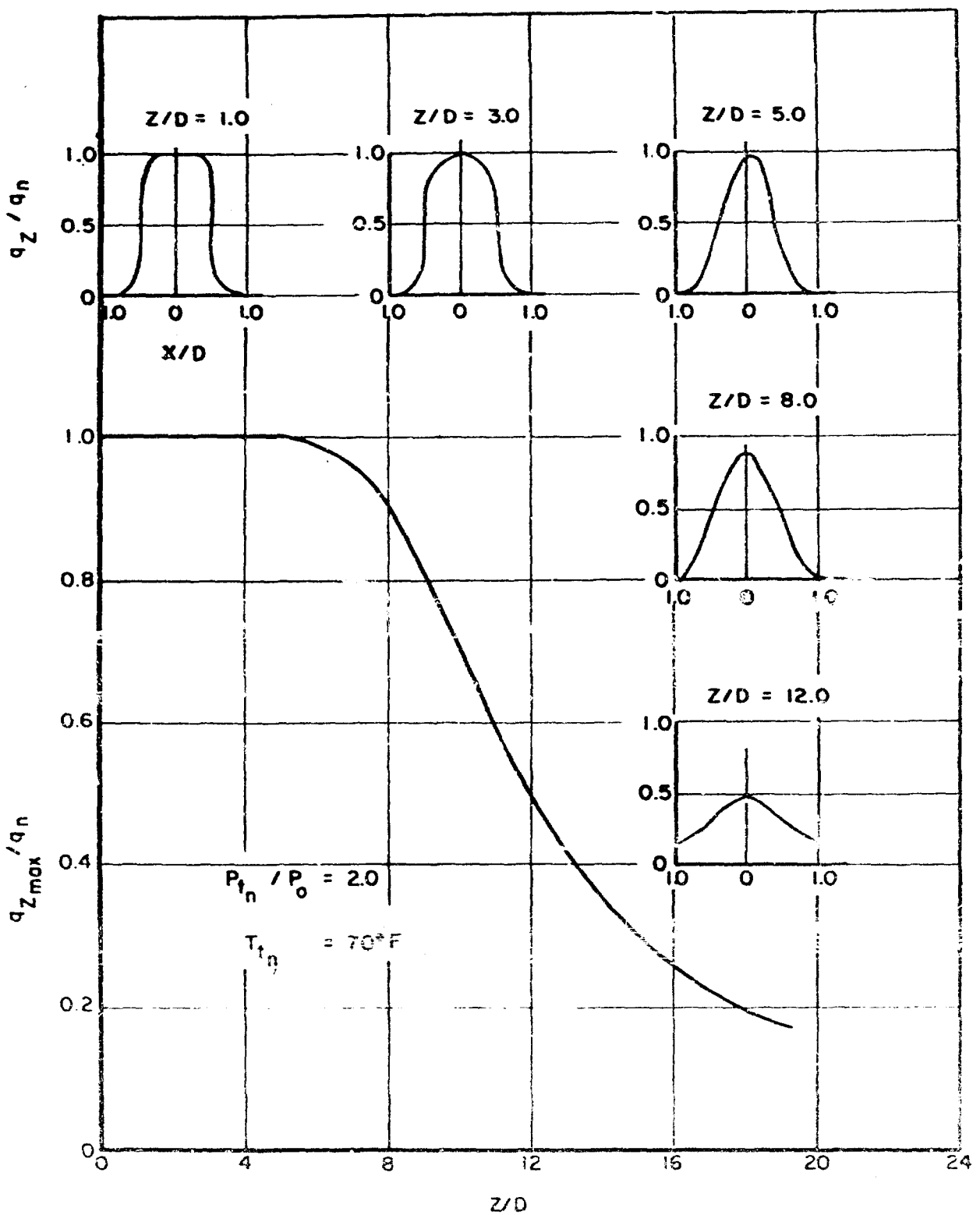

Figure 18. Dynamic Pressure Decay of a 1-Inch Circular Convergent Nozzle in Free Air

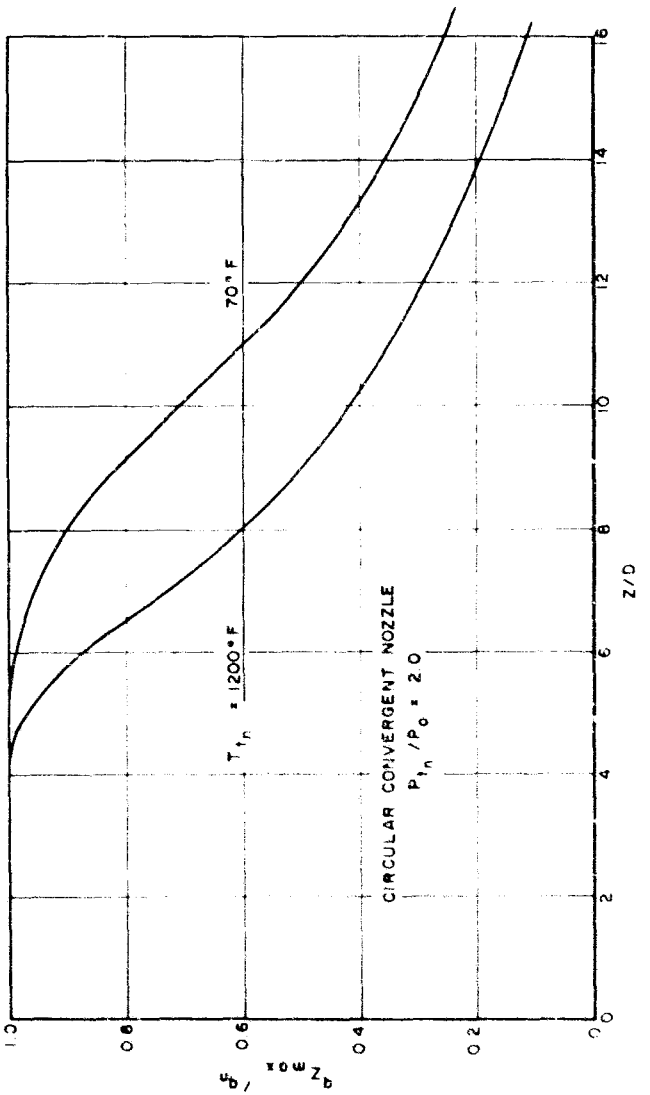

Figure 19. Jet Wake Dynamic Pressure Degradation at Two Exit Gas Temperatures In Free Air

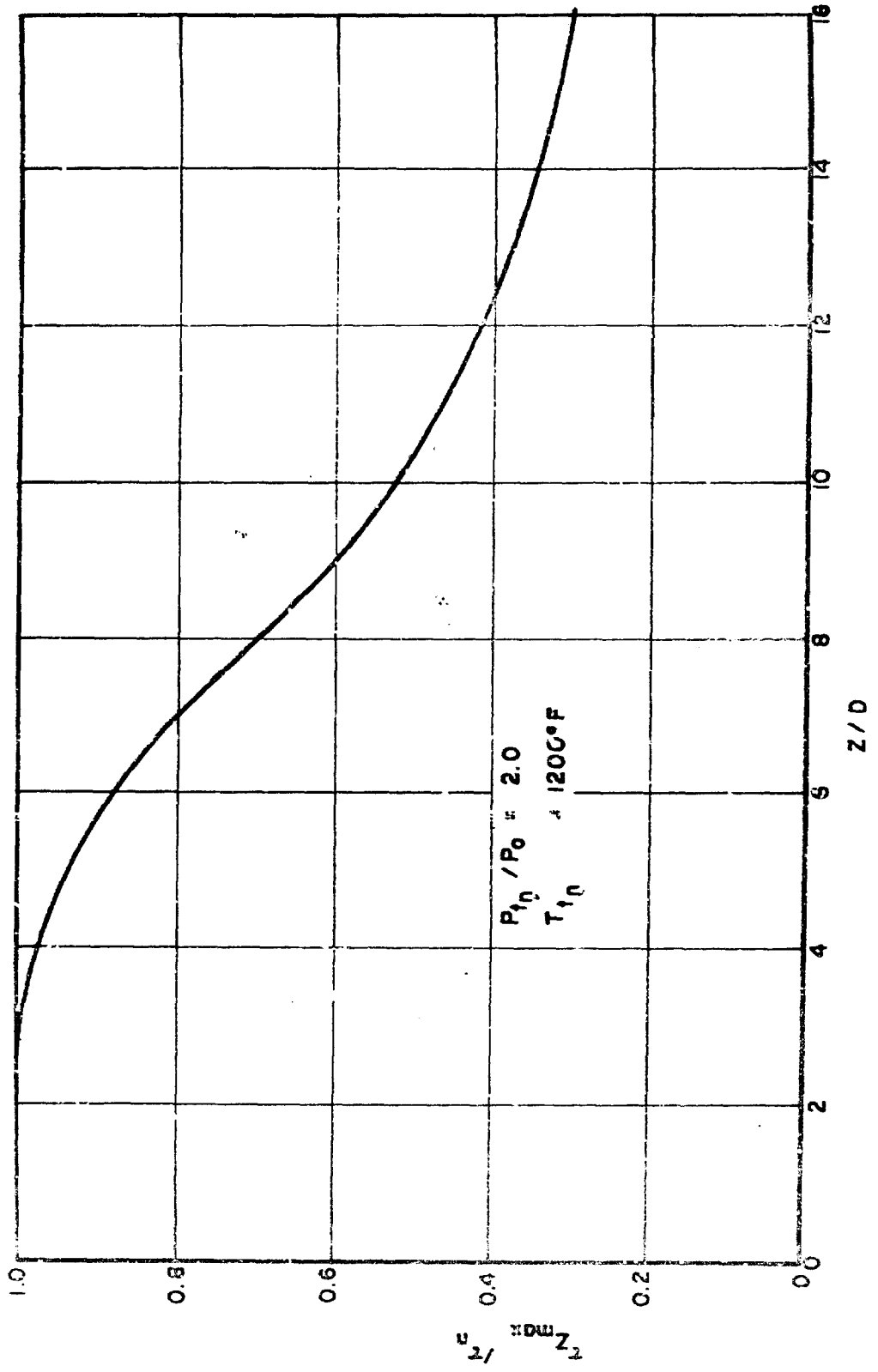

Figure 20. Jet Wake Differential Temperature Degradation for a Circular Convergent Nozzle in Free Air

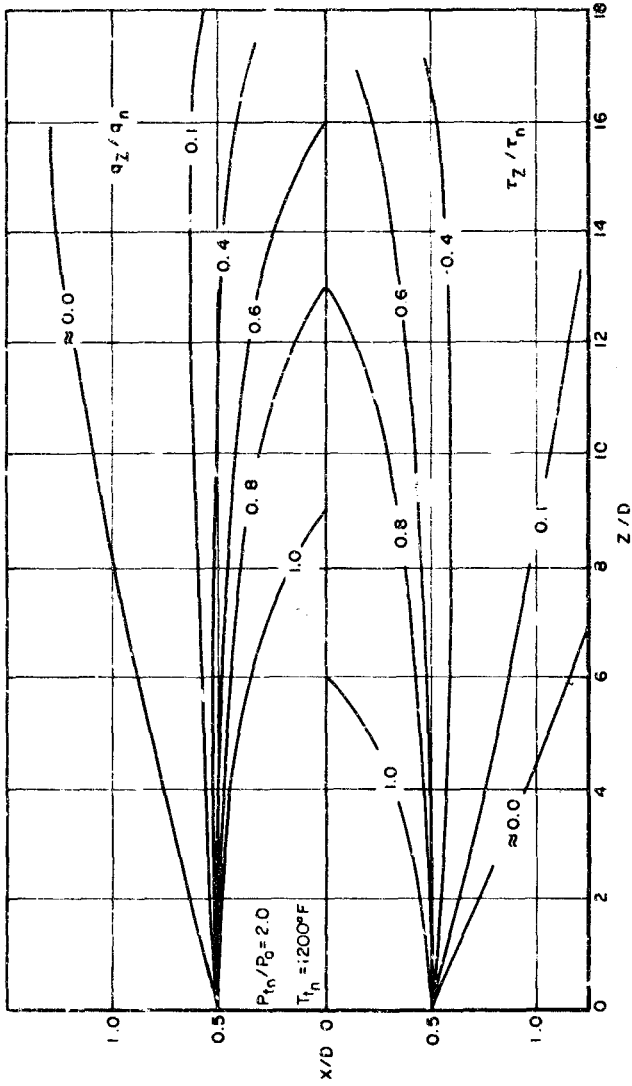

Figure 21. Jet Wake Dynamic Pressure and Differential Temperature Survey for a Circular Convergent Nozzle

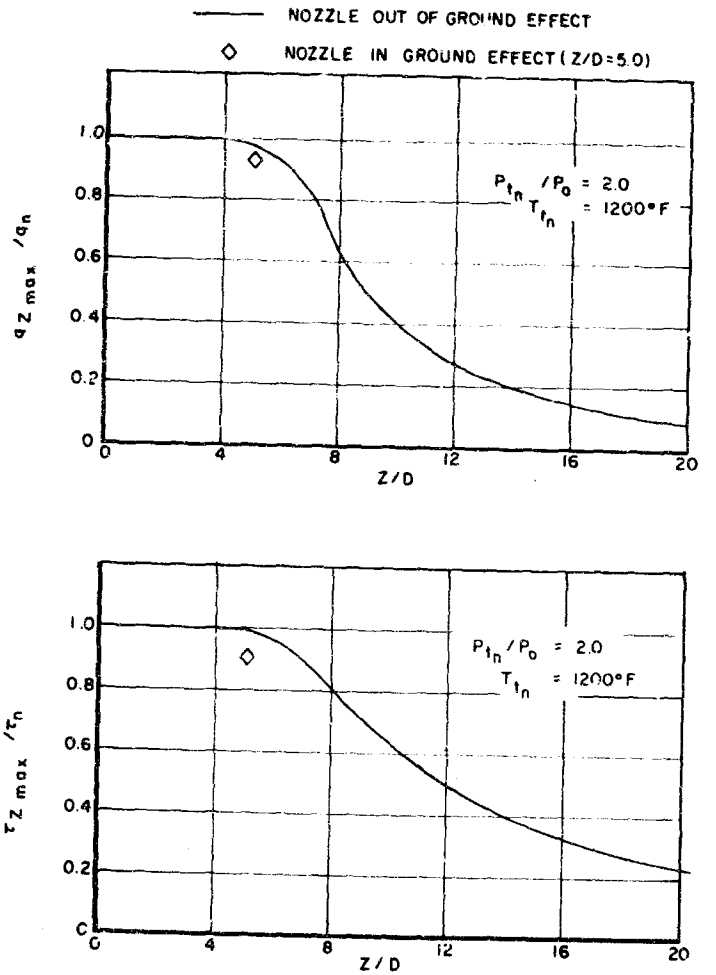

Figure 22. Effect of Ground Plane on Jet Wake Degradation Characteristics for a Circular Nozzle

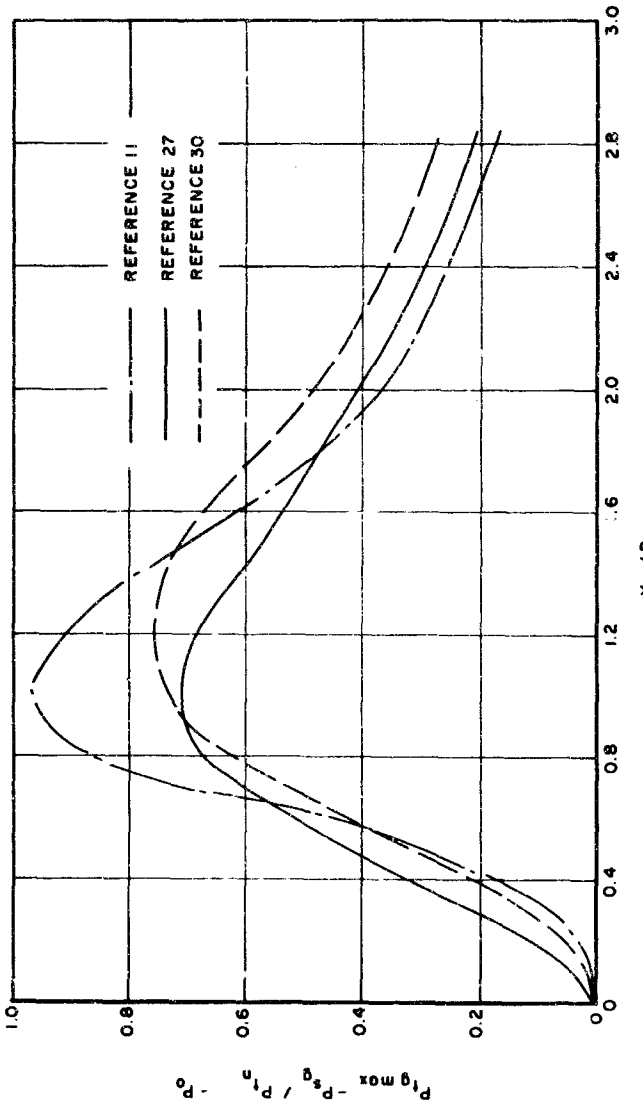

Figure 23. Radial Variation of Local Dynamic Pressure over the Ground Plane for a Circular Nozzle (from Various References)

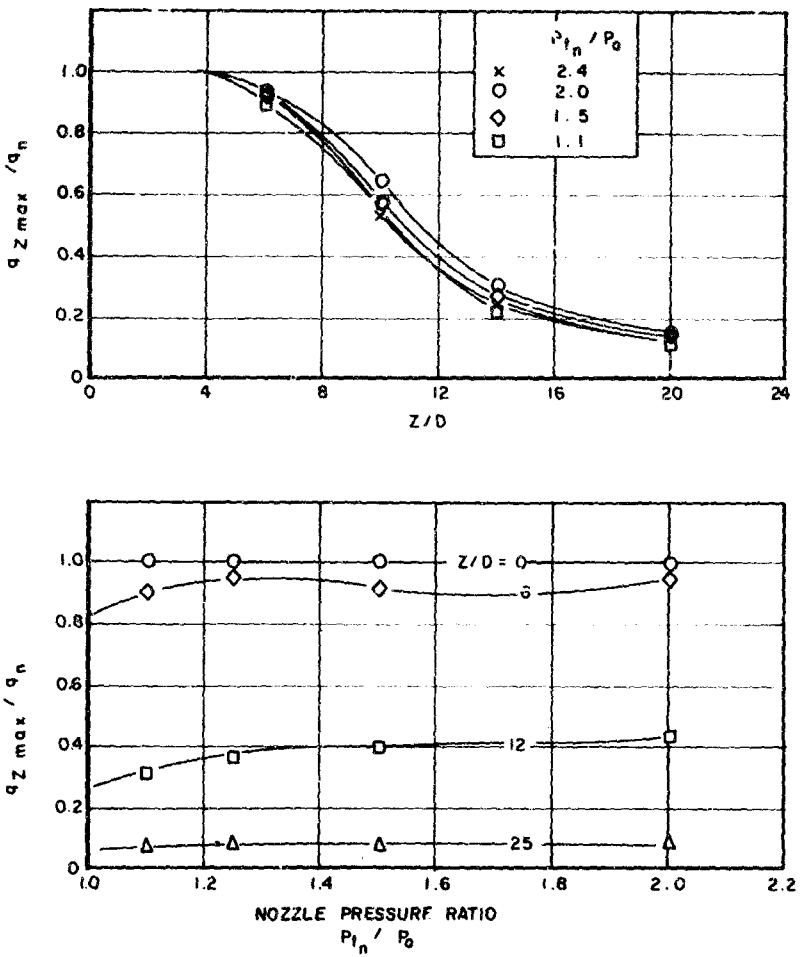

Figure 24. Jet Wake Pressure Degradation at Various Nozzle Pressure Ratios for a Circular Nozzle

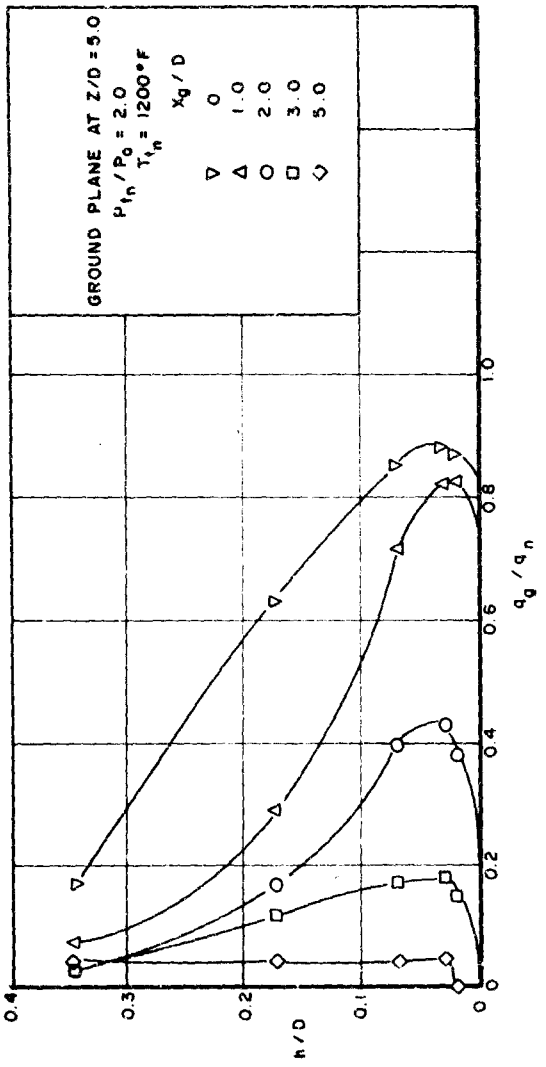

Figure 25. Pressure Profiles over the Ground Plane (q_g/q_n) for a Circular Nozzle

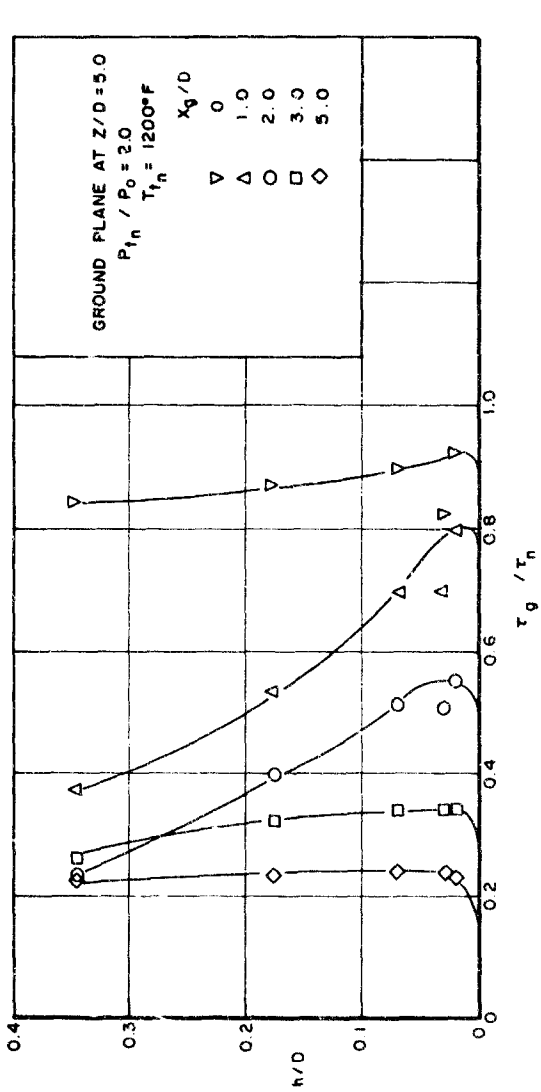

Figure 26. Differential Temperature Profiles (τ_g/τ_n) Adjacent to the Ground Plane for a Circular Nozzle

3. NEAR-GROUND OPERATIONAL PERFORMANCE

In almost all cases, jet nozzle operation within ground effect is unfavorable. Figure 33 shows lift losses are as high as 40% of the free air lift. The lower curve in Figure 33 shows this effect to be present out to a nozzle height of five diameters (the fuselage height and nozzle exit height are assumed to be the same). This test was conducted with an airplane model, and no separate breakdown of lift losses was determined; therefore, it is difficult to estimate the losses due to the engine itself. The negative pressure on the wings and fuselage due to the engine operation may contribute most of this lift loss.

The use of a perforated plate over the flat surface eliminated the "suckdown" effects until a height ratio of less than 3 was reached. Figure 34 shows the results of a suckdown test involving the use of a variable area circular plate located at the nozzle exit. The loss in lift does not appear unreasonable until plate-to-nozzle area ratios reach 30 or more. This loss represents the induced load on the plate due to the jet exiting under it and also represents the nozzle losses due to ground effect. It appears that the nozzle losses due to high back pressure are not affected until values of H/D of 3 or 4 are reached. Studies were also conducted on a four-jet and eight-jet configuration exiting under a delta wing model. The four and eight-jet configurations were located in rectangular patterns under the fuselage. Induced lift losses and the downwash decay pattern are shown in Figure 35. The eight-jet configuration shows the most rapid decay curve, but it also shows the greatest lift losses.

The near-ground operational performance of a rotor and ducted fan are shown in Figure 36. The rotor realizes the greatest benefit of near-ground operation, but this is not true for the ducted fan. Blade stall occurs at near-ground operation unless a very low blade angle is used, and a low blade angle would give very poor cruise performance if the engine is used for both lift and cruise. Likewise, if the optimum blade angle for cruise is used for take-off, a definite loss in lift would result.

The ground effect on several aircraft is shown in Figure 37. Propeller aircraft all benefit from operation near the ground. The four-propeller model benefits less than the two-propeller model because of the interference of the downwashes from adjacent engines. It also has smaller diameter propellers which could provide less induced lift. The X-14 deflected jet shows losses greater than 10% at fuselage heights of less than two. This is typical of most lift jets exiting near or under the fuselage.

4. GENERAL V/STOL ENGINE ENVIRONMENT AND AIRCRAFT PERFORMANCE DATA

Figure 38 shows the maximum range of operation of various V/STOL engines. Both the disc loading and slipstream temperatures are given for values at the exit of the propulsion system. Figure 39 indicates the point where ground erosion will commence for various type soils. Differences in these values may exist, depending on the amount of moisture and the relative configuration of the terrain.

In any discussion of V/STOL aircraft, certain performance parameters are always paramount in deciding as to what type vehicle to use for a particular mission. Several of these important parameters are presented in the final three figures. The hovering and cruise performance shown in Figure 40 is based on a consumption of fuel during hover of 3% of the aircraft gross weight; this would include hover for both take-off and landing. The helicopter offers the best hover performance but also the poorest cruising speed. The reverse is true of the turbojet, where hover times must be limited to 3 minutes or less.

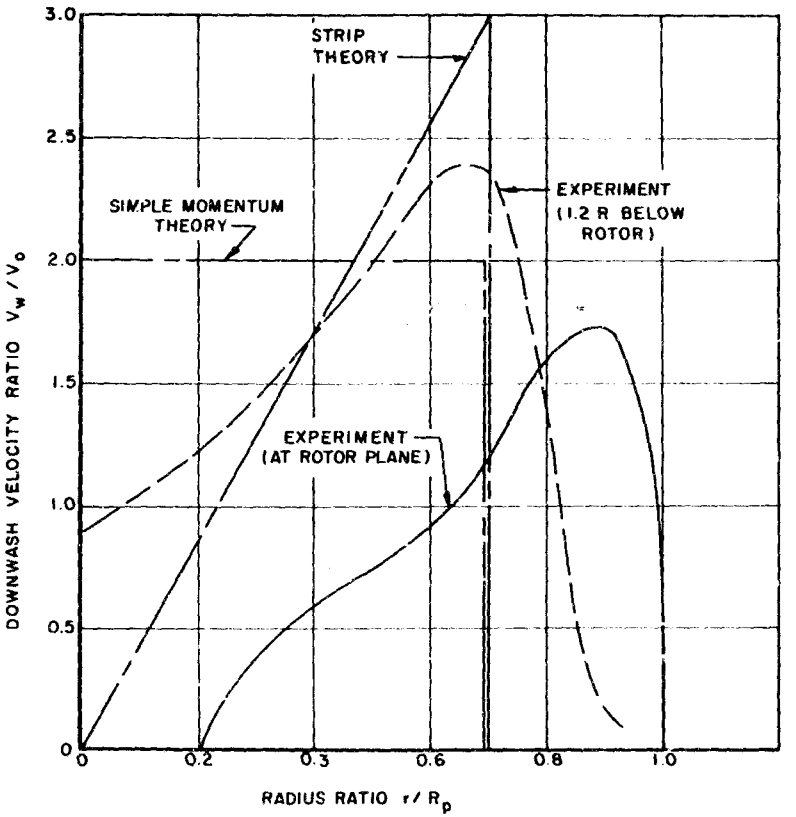

Figure 27. Comparison Between Theoretical and Experimental Downwash Velocities for a Rotor in Free Air

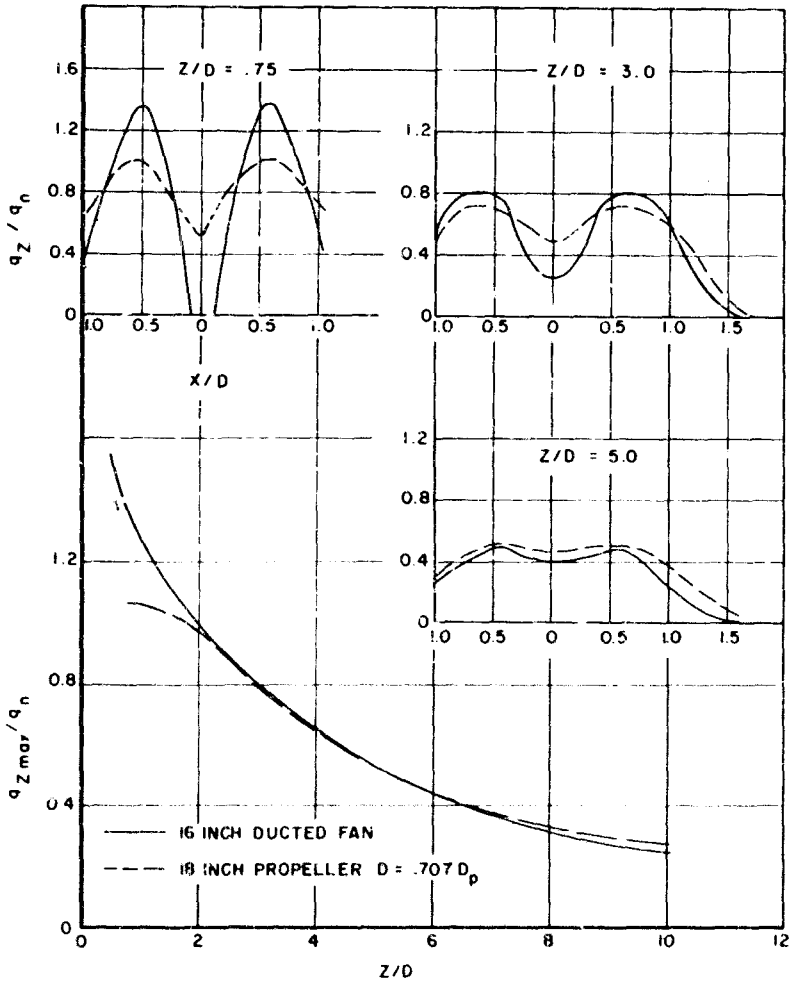

Figure 28. Dynamic Pressure Decay and Slipstream Profile of a Propeller and a Ducted Fan in Free Air

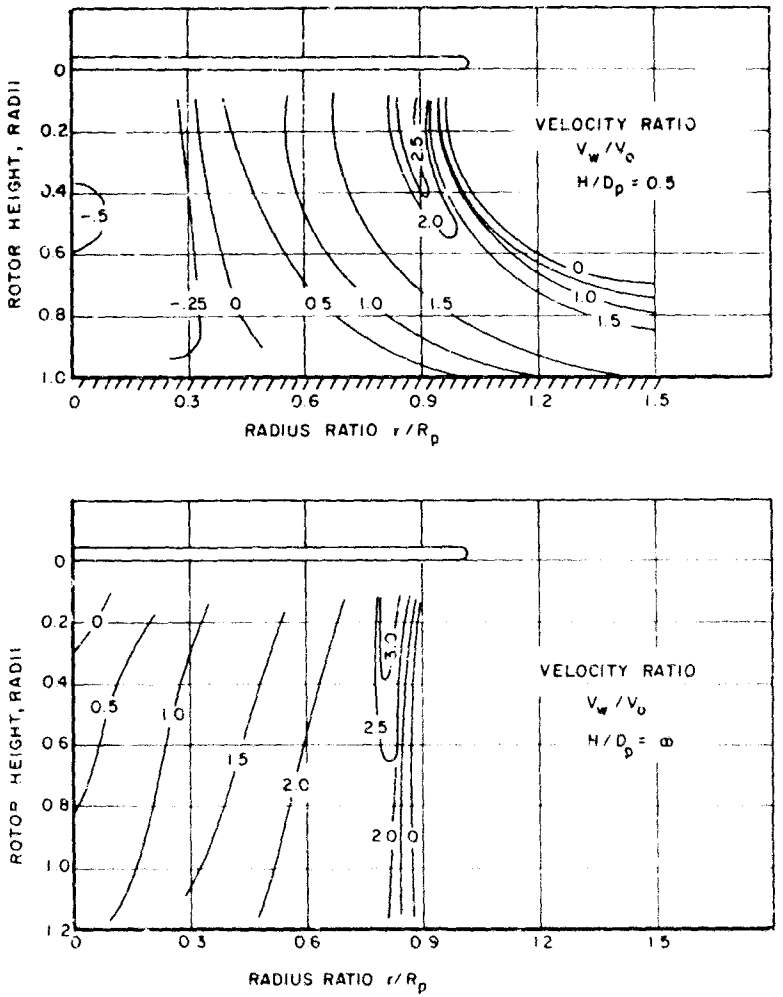

Figure 29. Velocity Contour Map for a Rotor in Ground Effect and in Free Air

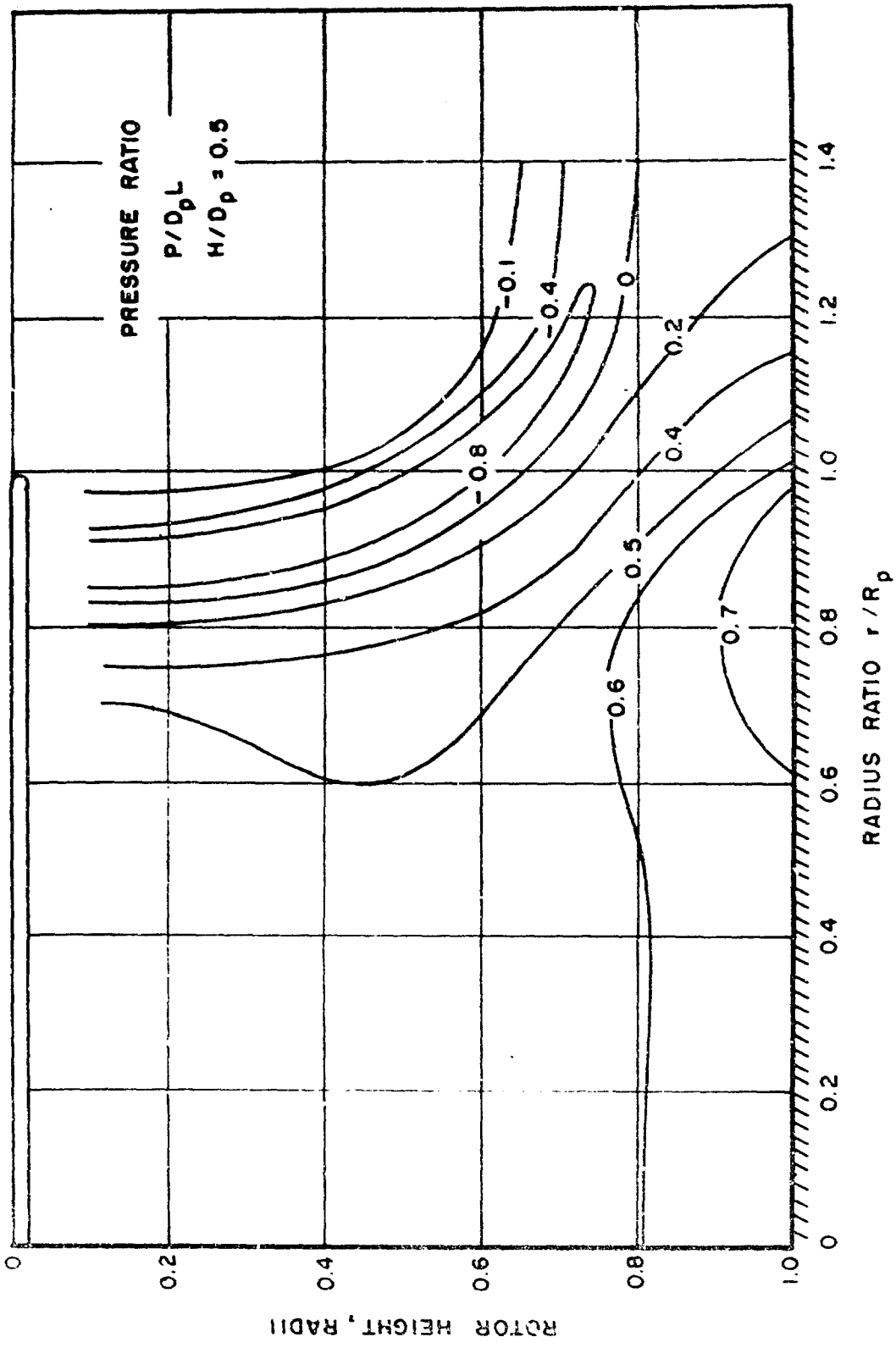

Figure 30. Static Pressure Distribution for a Rotor 1.0 Radius Above Ground

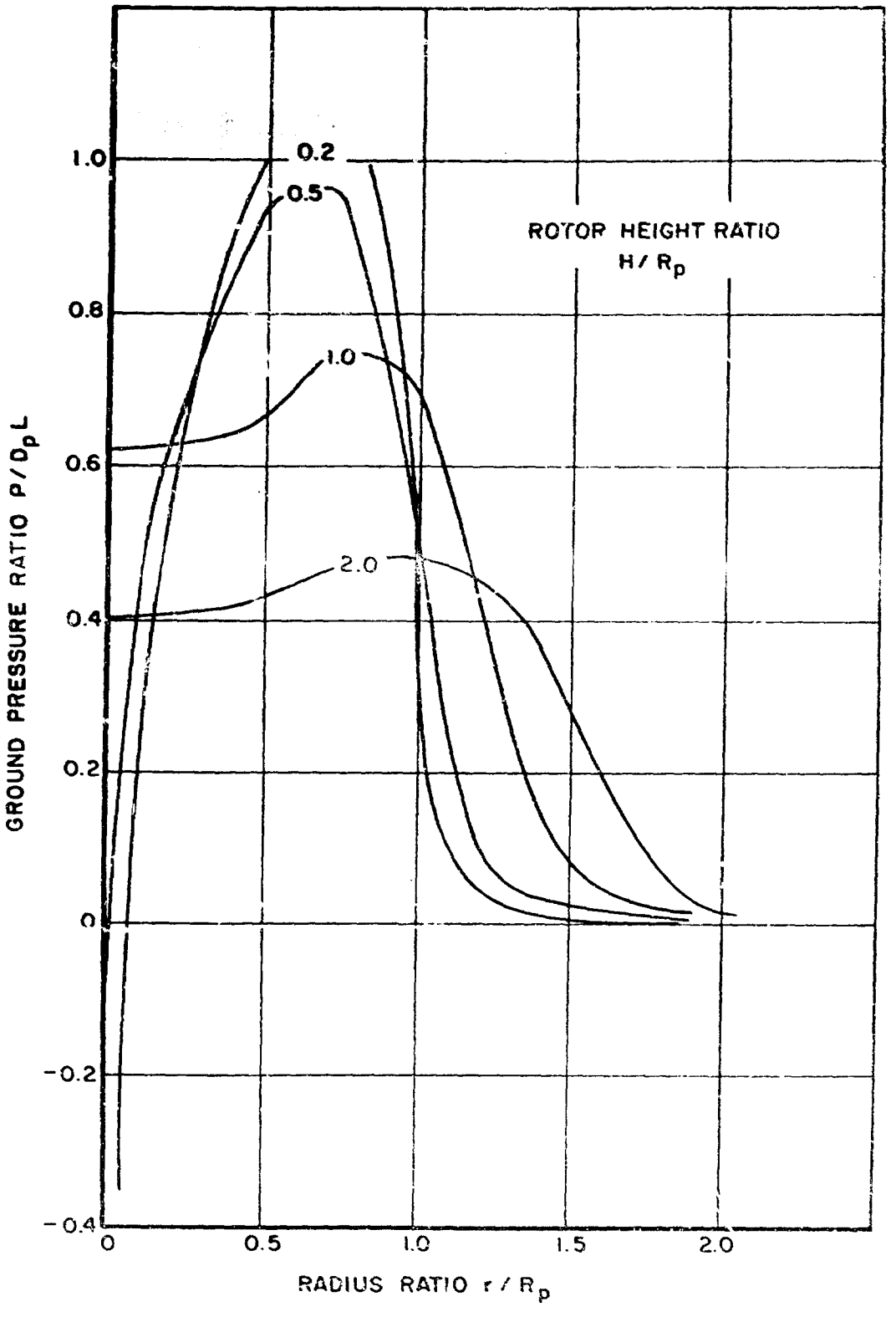

Figure 31. Ground Static Pressure for Various Rotor Heights

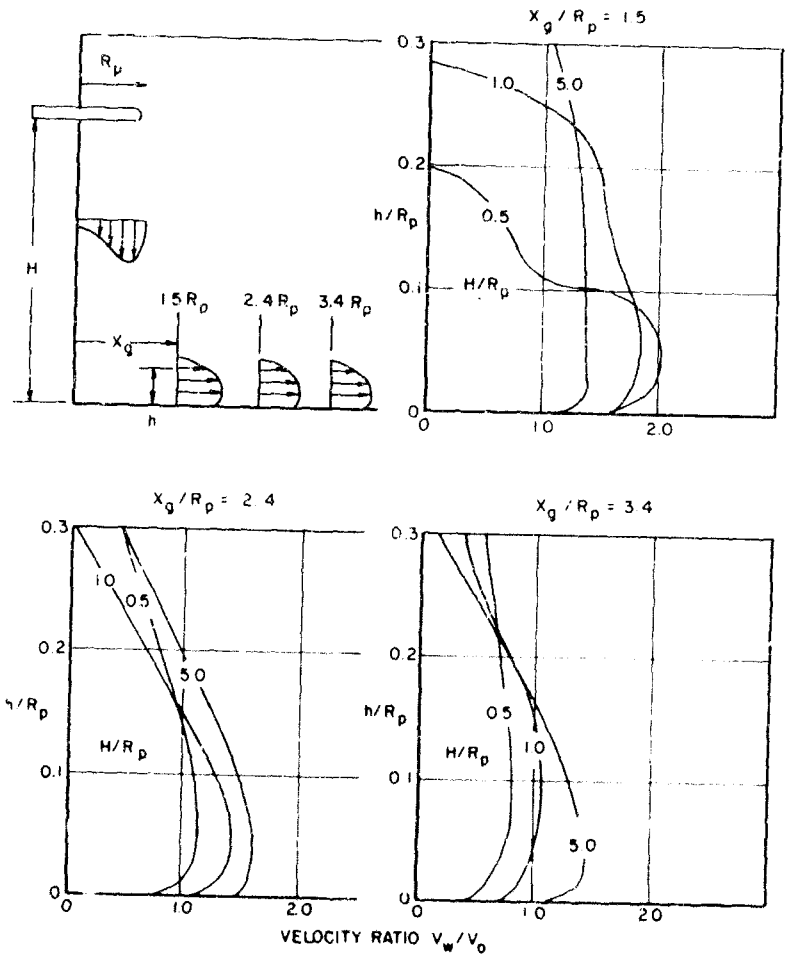

Figure 32. Ground Velocity Profiles at Various Rotor Heights for Different Ground Stations

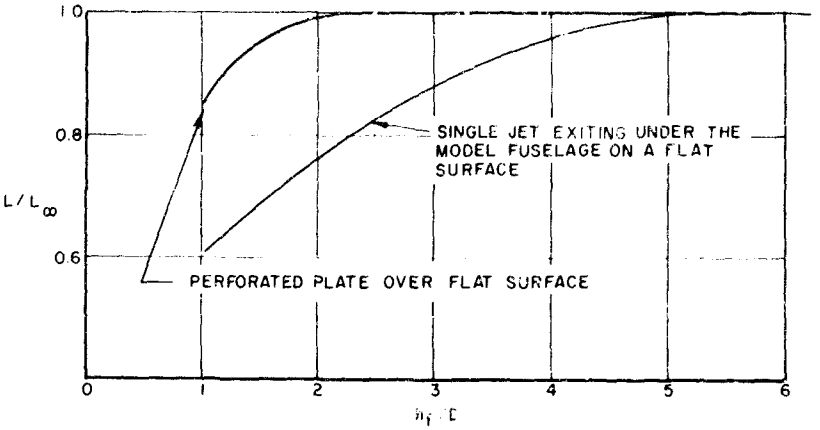

Figure 33. Effect of Near-Ground Operation on a Single-Jet-Model Configuration

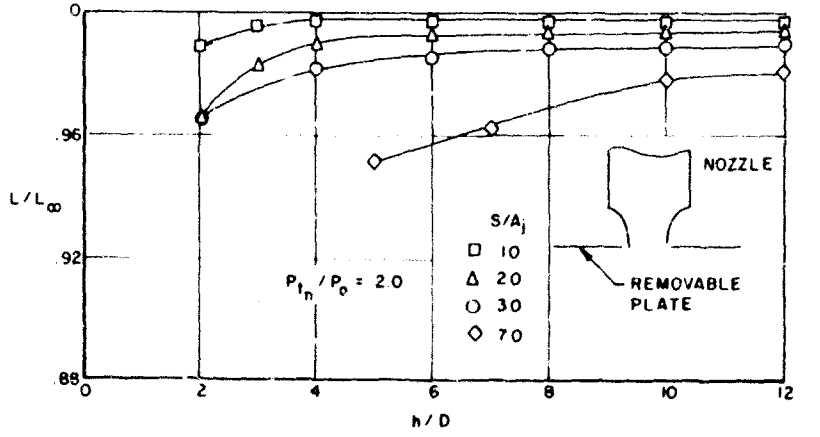

Figure 34. Effect of Nozzle Height on Lift Losses for Various Circular Planform Plate Areas

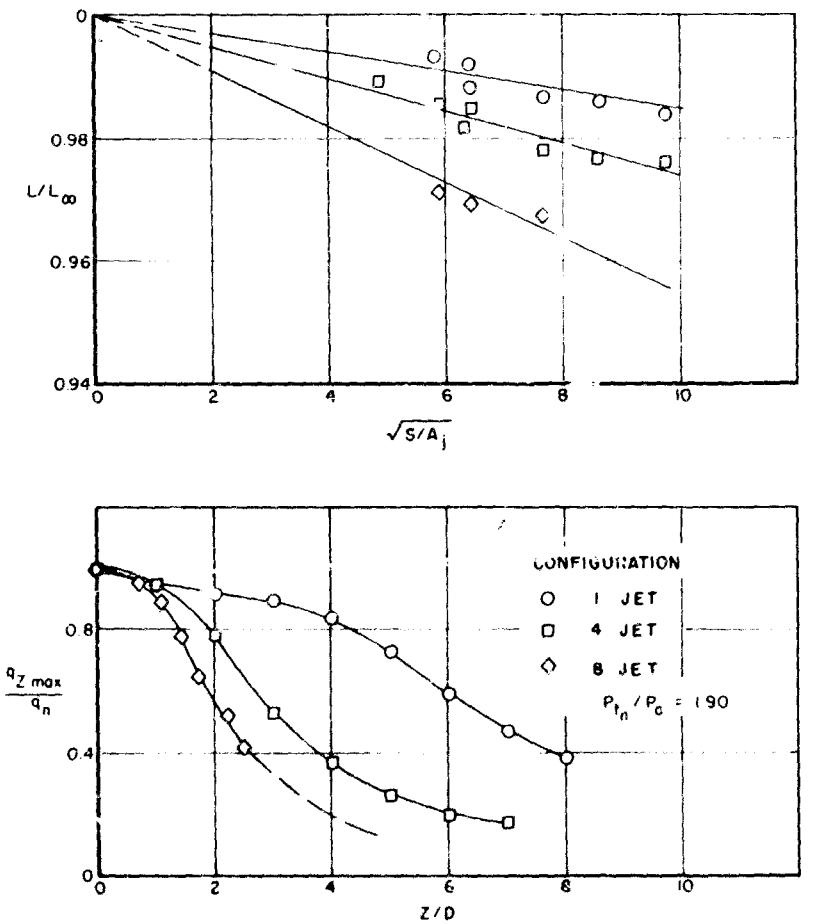

Figure 35. Induced Load on Several Planform Plates and Pressure Decay for Single and Multiple Jet Configurations in Free Air

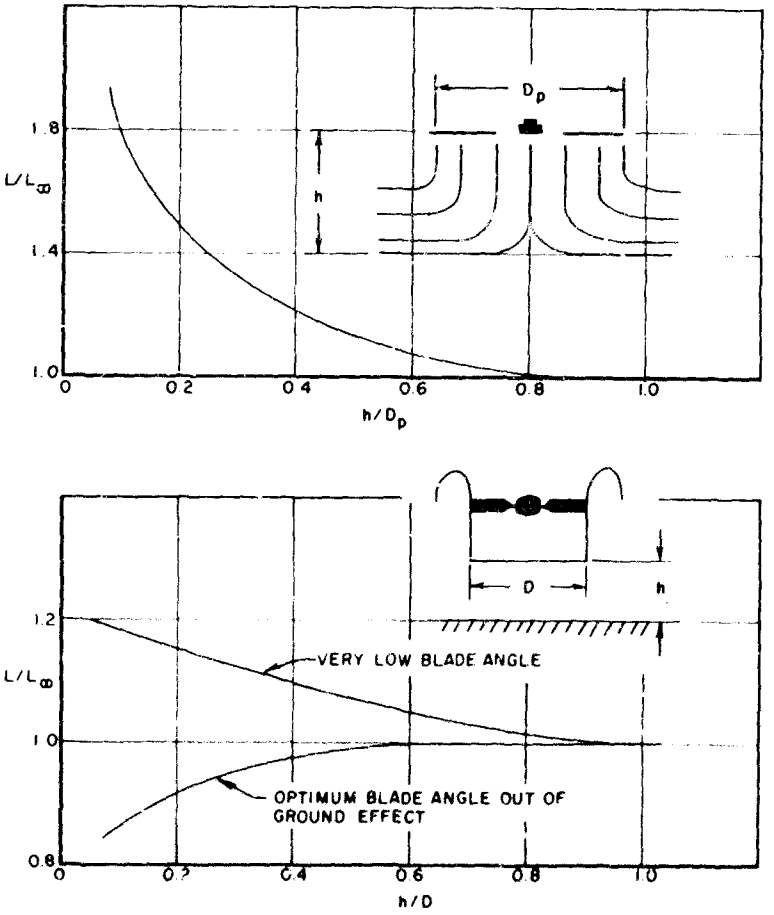

Figure 36. Variation in Lift of a Propeller or Rotor and a Ducted Fan Near the Ground

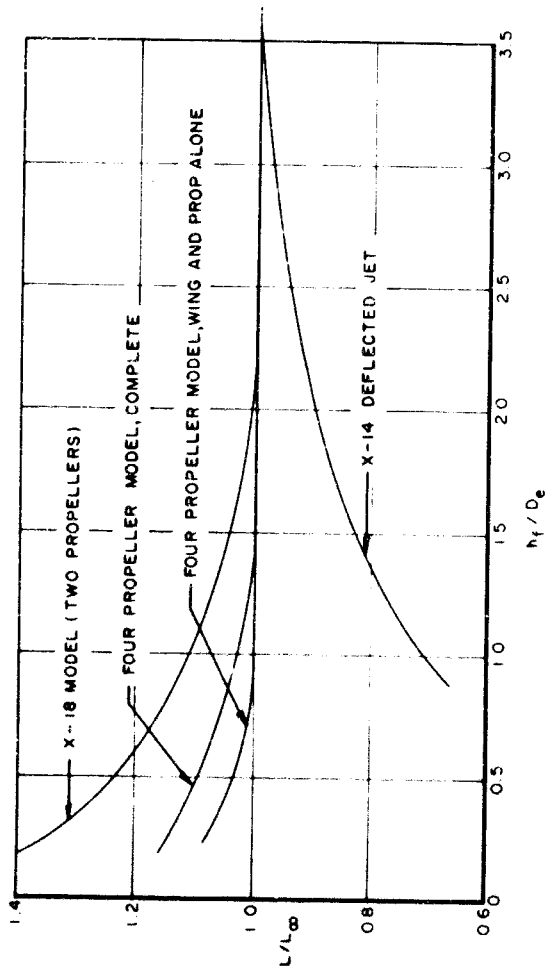

Figure 37. Effect of Ground on Various Aircraft Configurations and Types

A possible trade-off between these two extremes is shown in Figure 41. This comparison is for an overload condition of 20% above that of VTOL weight. The rotor configurations have relatively high take-off distances because of the low power requirement in hovering and the low variation in power with speed. The tilt duct and flapped tilt wing make use of the highly efficient wing for needed lift, while the remaining types suffer from problems such as short wing span and poor load distribution during transition in take-off and landing. The final figure, Figure 42, indicates the fuel consumption required in hovering. The amount of fuel consumed by the turbojet for a hover time of one hour approaches the weight of the aircraft. The rotor aircraft shows the best performance where hover times of several hours may be required.

5. SUMMARY OF V/STOL AIRCRAFT SPECIFICATIONS

Table I provides a listing of the latest specifications for V/STOL aircraft (including helicopters). This is provided not only as a general source of information but also as a reference for specific aircraft dimensions for use in Sections II and III of this report. All of the information contained here has been taken from "Janes' - All the World's Aircraft," 1964 thru 1966 editions.

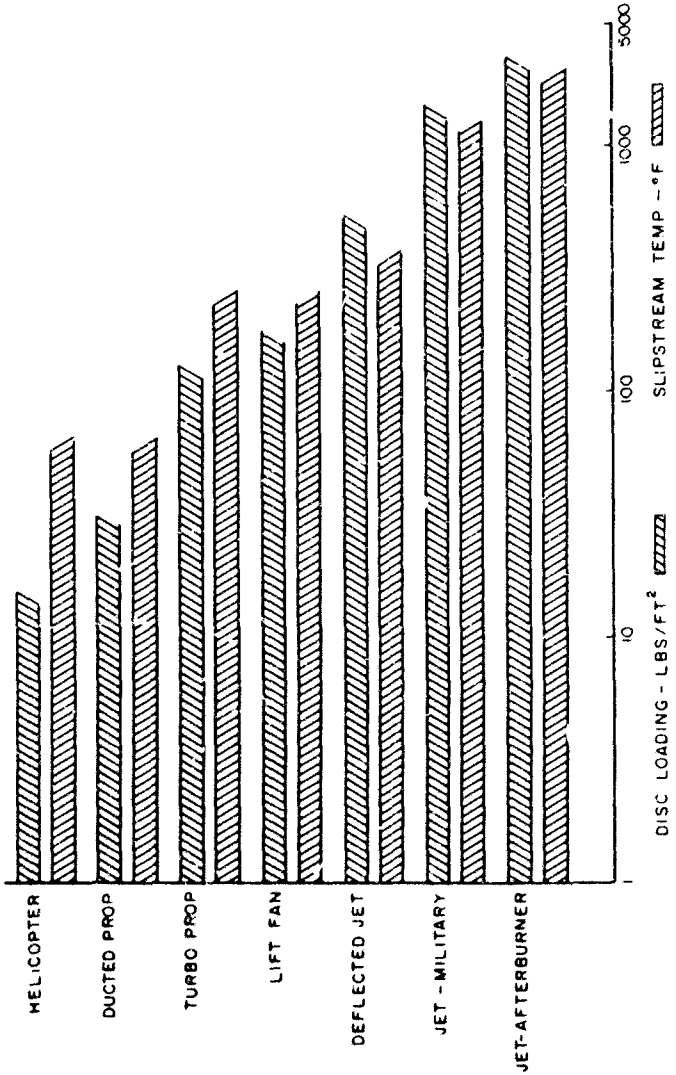

Figure 38. Aircraft Engine Downwash Environment

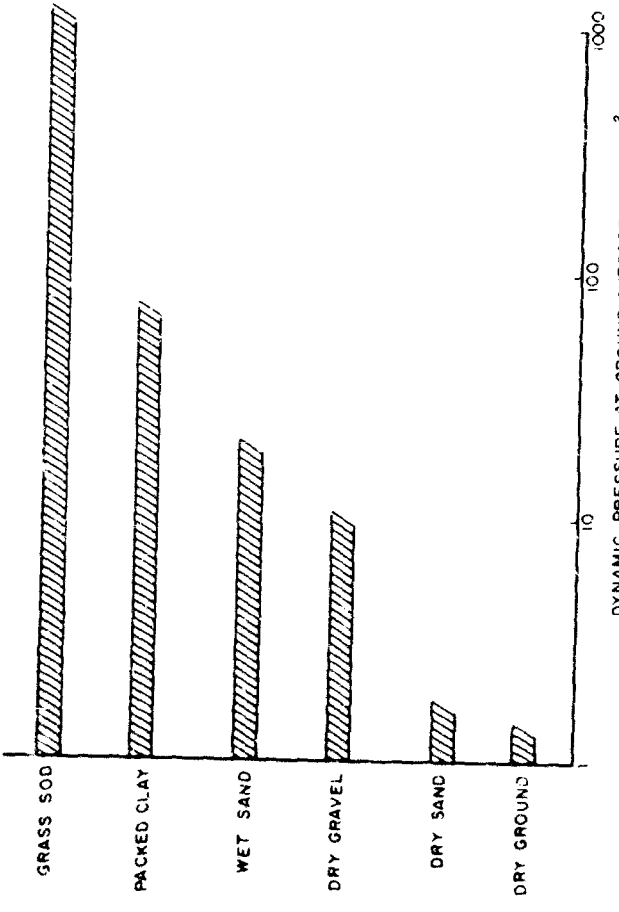

Figure 39. Terrain Resistance to Overpressure

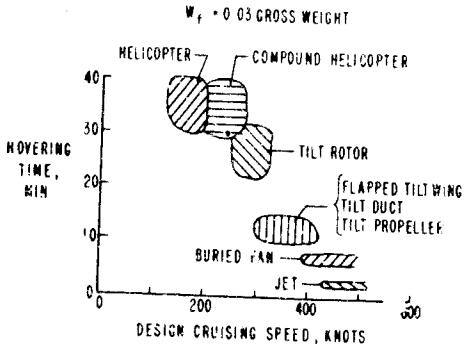

Figure 40. Hovering and Cruise Performance

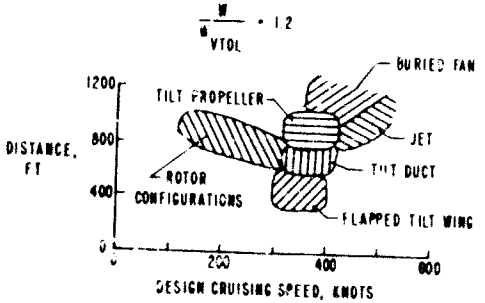

Figure 41. STOL Performance - Takeoff Distance over a 50-Foot Obstacle

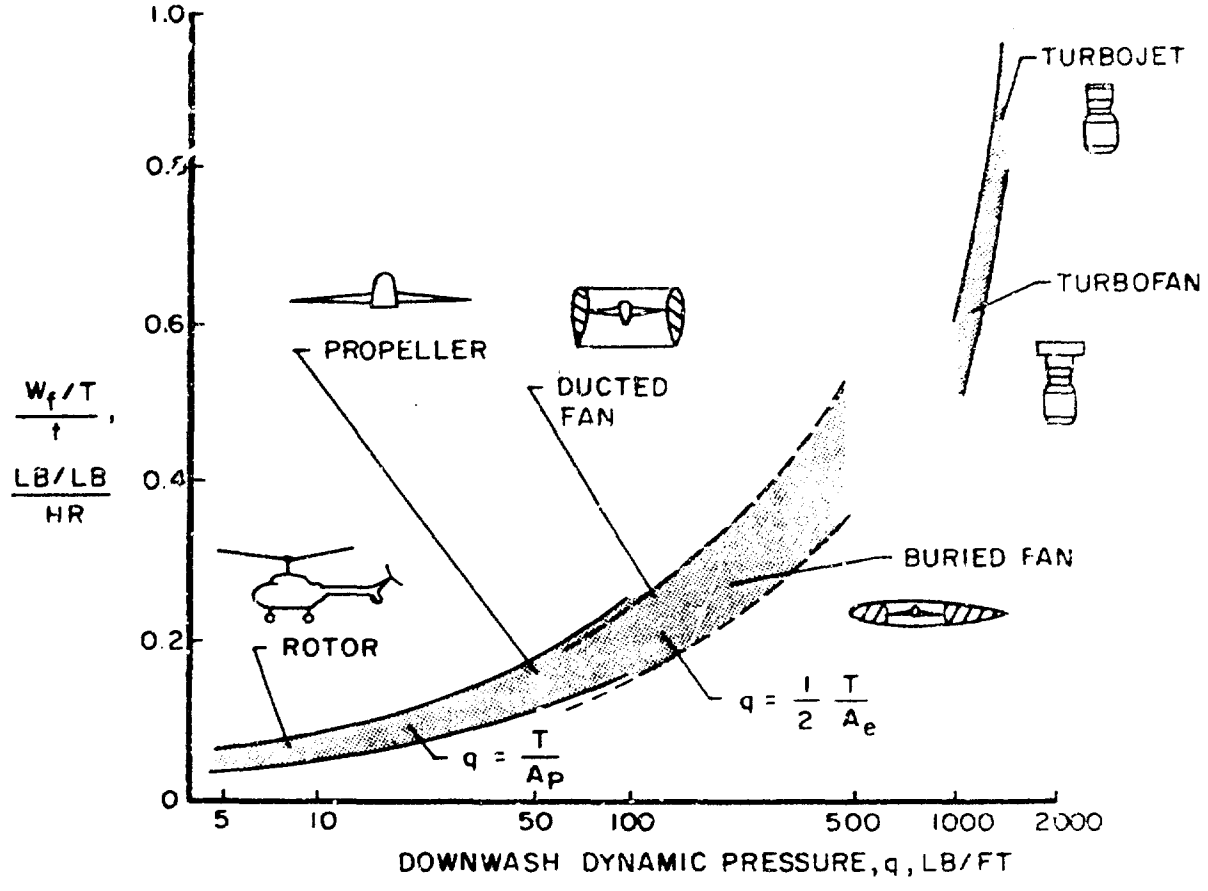

Figure 42. Fuel Consumption in Hovering

TABLE I

SUMMARY OF SPECIFICATIONS FOR V/STOL AIRCRAFT

Type	Designation	Use	Main Rotor Dia.	Main Rotor Ht.	Empty Wt. (lbs)	Max. T.O. Wt. (lbs)	Max. Speed (mph)
Bell (Single Rotor)	Model 47 USAF(UH-13) Army (OH-13)	Utility	37'1½"	9'3"	1713	2850	105
	Model 204 Army (UH-1)	Utility	44'	14'	4502	8500	138
Hiller (Single Rotor)	Model E-4 Army (UH-12)	Utility	35'5"	9'10"	1813	2800	96
Kaman (Single Rotor)	Model UH-2 Army (UH-24)	Utility and Rescue	44'	12'	6100	10,920	162
Sikorsky (Single Rotor)	Model S-56 Army, Navy Marine (CH-37)	Transport	72'	22'	20,690	31,000	130
	S-58 Army, Navy Marine H-34 (CH-34)		56'	16'	7630	13,000	123
	S-61 CH-3C (HH-3C)	Assault Transport	62'	16'	11,933	22,000	165
	S-62 Coast Guard (HH-52A)	Search & Rescue	53'	14'2"	4789	8300	109
	S-64A (Skycrane CH-54A)	Heavy Flying Crane	72'	18'7"	17,240	38,000	117
	S-65A (Sea Stallion CH-53A)	Heavy Assault Transport	72'	16'6"	20,950	38,950	200+
Boeing Vertol (Dual Rotor)	Model 107 Marine CH-46A	Transport	Front-50' Rear-50' Rotor ℄ Distance-33'4"	Front-14'3" Rear-16'10"	9600	19,000	168
	Model 114 Army CH-47A	Transport	Front-59' Rear-59' Rotor ℄ Distance-39'6"	Front-17' Rear-18'6"	17,559	33,000	175

TABLE I (Continued)

Type	Use	Engine Data	Propulsion Device	Max. VTOL T.O. Wt. (lbs)	Max. STOL T.O. Wt. (lbs)	Max. Speed
Hawker Siddley P.-1127 (Vectored Thrust -bypass jet)	Tactical Strike Fighter	1-Turbofan engine at 15,200 lbs. thrust each (military)	2-Fwd nozzles @1.11' dia. ea. 2-Aft nozzles @.94' dia. ea. Exit nozzle height ≅ 5.0'	12,400	15,500	Mach = .87
Bell X-14 (Vectored Thrust)	Experimental Research Aircraft	2-GE J-85-5 turbojet at 2650 lbs. thrust each (military)	Vectored thrust nozzles 2 Lift nozzles @1.5' dia. ea. 2 Cruise nozzles @1.5' dia. ea. Exit nozzle height ≅ 3.5'	3900	N/A	Mach = .5
EWR VJ-101C (Direct Thrust)	Single seat Fighter	6-RB.145 lift jets at 2750 lbs. thrust each (military) 2-Each wingtip 2-Fuselage	4-Wingtip nozzles @1.25' dia. ea. 2-Fuselage nozzles @1.0'dia. ea. Wingtip engines ℄ dist = 20' Exit nozzle ht. ≅ 4.0'	13,250	N/A	Mach = 1.05
Dassault Mirage III-V (Direct Thrust)	Single seat Mach 2 Fighter	8-BD.162 lift jets at 4650 lbs. thrust each (military) 1-TF106 turbofan rated at 20,500 lbs thrust with AB.	8-lift jet nozzles @1.25' dia. each. 2-Fuselage engine pods @4 engines each. Exit nozzle ht 5.0'	29,630	N/A	Mach = 2.15
Ryan XV-5A (Ducted fan)	Research VTOL Aircraft	2-GE J-85-5 turbojets at 2658 lbs. thrust each (military)	2-Inwing lift fans at 5'2½" dia. each. Total lift per fan = 6978 lbs. Fan exit ht. ≅ 4.0'	12,300	13,600	Mach = .70
LTV XC-142 (Tilt Wing Turboprop)	Transport	4-GE T64-4 turboshaft engines	4 Propellers @15'6" dia. each Rotor height = 15' Distance between outboard engine centerlines = 53'	37,373	44,500	409 mph
Bell X-22A (Tilt ducted prop)	V/STOL Research Aircraft	4-GE T58-8 turboshaft engine	4-7' diameter ducted propellers. Fwd prop ℄ distances = 23' Rear " " " = 40' Fwd prop height = 7' Rear " " = 9'	15,980	17,680	325 mph

REFERENCES

1. Keuthe, A.M., "Investigations of the Turbulent Mixing Regions Formed by Jets." Journal of Applied Mechanics 2, No. 3, September 1935, pp. A87-95.

2. Wolfe, G.W., VTOL Downwash Study - Part I of the Free Jet Analysis, CVA AER-EOTM-53, dtd 14 Sept 1960.

3. Schlichting, H., Boundary Layer Theory, McGraw Hill Book Co., Inc., 1955, pp. 159-162, 500-502.

4. Squire, H.B. and Trouncer, J., Round Jets in a General Stream, British ARC R & M 1974, 1944.

5. Wolfe, G.W. And Walker, S.C., "Results of a Small Scale Downwash Test Program," CVA EOR-13108 dtd 7 Dec 1960.

6. Pai, Shih I, Fluid Dynamics of Jets, D. Van Nostrand Company, 1954, pp. 7-9, 78-79.

7. O'Neal, G.B., "A Method of Calculating VTOL Aircraft Landing Mat Size," 2-53910/5TM-7, 22 April 1965.

8. Murray, R.I., et.al., "Deflection of a Jet by a Normal Wall." Am. Soc. of Civil Engineers. Proc. 82 (Hydraulics 4 No. 1038), Aug 1956, pp. 26-29.

9. Poreh, M. and Cermack, J.E., "Flow Characteristics of a Circular Submerged Jet Impinging Normally on a Smooth Boundary," Sixth Conf. on Fluid Mechanics, 1959. The Univ. of Texas, pp. 198-207.

10. Bradshaw, P. and Love, Edna M., "The Normal Impingement of a Circular Air Jet on a Flat Surface," Aeronautical Research Council A.R.C. 21, 268, F.M. 2856, P.L. 20, Sept 18, 1959 (CVA Lib. No. 45,884).

11. Kuhn R.E., An Investigation to Determine Conditions Under Which Downwash from VTOL Aircraft Will Start Surface Erosion from Various Types of Terrain, NASA TN D-56, Sept. 1959.

12. Galuert, M.B., "The Wall Jet," Journal of Fluid Mechanics, Vol. 1, Part 6, Dec 1956, pp. 625-643.

13. Bakke, P., "An Experimental Investigation of a Wall Jet." Journal of Fluid Mechanics, Vol. 2, Part 5, July 1957, pp. 467-472.

14. Isely, F.D. and Wolfe, G.W., A Method of Calculating The Airflow Field Resulting from VTOL Aircraft Downwash, LTV-AER-EOR-13112, 12-29-60.

15. Wolfe, G.W. and Walker, S.C., Results of a Small Scale Downwash Test Program, LTV-EOR-13108, 12-7-60.

16. Brady, G.W. & Ludwig, G., "Theoretical and Experimental Studies of Impinging Uniform Jets," IAS Paper 63-23, Jan 1963.

17. Newsom, W.A. & Tosti, L.P., Slipstream Flow Around Several Tilt Wing VTOL Aircraft Models Operating Near the Ground, NASA TND-1382, Sept., 1962.

REFERENCES (CONT'D)

18. Higgins, C.C. & Wainwright, T.W., Dynamic Pressure & Thrust Characteristics of Cold Jets Discharging From Several Exhaust Nozzles Designed for VTOL Downwash Suppression, NASA TND-2263, April 1964.

19. Turner, G.D., The Interaction of Two Parallel Sonic Jets Impinging on a Flate Plate, M.S. Thesis, University of Texas, Jan. 1965.

20. Kuhn, R.E., & McKinney, Marrion O., NASA Research on the Aerodynamics of Jet VTOL Engine Installations, AGARD Specialist Meeting on Aerodynamics of Power Plant Installation, Tullahoma, Tennessee, 25-27 October 1965.

21. Colin, P.E., Ground Proximity and the VTOL Aircraft, North Atlantic Treaty Organization AGARD Report No. 409, 1962.

22. Frandenburgh, E.A., Flow Field Measurements for a Hovering Rotor Near the Ground. A.H.S. 5th Annual Western Forum, Los Angeles, California, September 1958.

23. Rolls, L. Stewart, Jet VTOL Power Plant Experience During Flight Test of X-14 VTOL Research Vehicle, AGARD Specialists Meeting on Aerodynamics of Power Plant Installation, Tullahoma, Tennessee, 25-27 October 1965.

24. O'Bryan, Thomas C., An Investigation of the Effect of Downwash From a VTOL Aircraft and a Helicopter in the Ground Environment, NASA TND-977, Langley Research Center, Langley Air Force Base, Virginia, October 1961.

25. Heyson, Harry H., An Evalustion of Linearized Vortex Theory as Applied to Single and Multiple Rotors Hovering In and Out of Ground Effect, NASA TND-43, Langley Research Center, Langley Field, Virginia, September 1959.

26. Schade, Robert O., Ground Interference Effects, NASA TND-727, Langley Research Center, Langley Field, Virginia, April 1961.

27. Higgins, C.C., Kelly, D.P., & Wainwright, T.W., Exhaust Jet Wake Characteristics of Several Nozzles Designed for VTOL Downwash Suppression, NASA CR-373 January 1966.

28. Gentry, Carl L. & Margason, Richard J. Jet Induced Lift Losses on VTOL Configurations Hovering In and Out of Ground Effect, NASA TND-3166, February, 1966.

29. Kuhn, Richard E., Review of Basic Principles of V/STOL Aerodynamics, NASA TND-733, March 1961.

30. Toni, Itero and Komatsu, Yasuo, Impingement of a Round Jet on a Flat Surface, Presented at the Eleventh International Congress of Applied Mechanics, Muchen 1964.

UNCLASSIFIED
Security Classification

DOCUMENT CONTROL DATA - R&D

(Security classification of title, body of abstract and indexing annotation must be entered when the overall report is classified)

1 ORIGINATING ACTIVITY (Corporate author)	2a REPORT SECURITY CLASSIFICATION
Air Force Aero Propulsion Laboratory Wright-Patterson AFB, Ohio 45433	UNCLASSIFIED 2b GROUP

3 REPORT TITLE

A Rapid Analytical Method of Determining General Downwash Flow Field Parameters for V/STOL Aircraft

4 DESCRIPTIVE NOTES (Type of report and inclusive dates)

5 AUTHOR(S) (Last name, first name, initial)

Hohler, David J.

6 REPORT DATE	7a TOTAL NO. OF PAGES	7b NO. OF REFS
November 1966	71	30

8a CONTRACT OR GRANT NO	9a ORIGINATOR'S REPORT NUMBER(S)
b PROJECT NO 8174	AFAPL-TR-66-90
c Task No. 817401	9b OTHER REPORT NO(S) (Any other numbers that may be assigned this report)
d	

10 AVAILABILITY/LIMITATION NOTICES This document is subject to special export controls and each transmittal to foreign governments or foreign nationals may be made only with prior approval of the Support Technology Division, Air Force Aero Propulsion Laboratory, W-PAFB, Ohio

11 SUPPLEMENTARY NOTES	12 SPONSORING MILITARY ACTIVITY
	Air Force Aero Propulsion Laboratory Wright-Patterson Air Force Base, Ohio

13 ABSTRACT

This report presents a method of analytically determining the general downwash flow field parameters of various types of V/STOL aircraft. The basic difference between the operation of V/STOL aircraft and conventional aircraft is their method of take-off and landing. During these operations, V/STOL aircraft produce high downwash air velocities that impinge and spread out over the surface of the ground. Depending on the size, type, and number of engines on the aircraft, this downwash can cause damage to nearby aircraft, equipment, or personnel. Past theoretical methods based on incompressible flow theory have been unsuccessful in establishing a means of computing this downwash flow field. A combined method, however, of proven experimental data and certain analytical approaches have yielded a useful means of predicting the general downwash flow field parameters. This report presents these approaches and demonstrates their usefulness.

DD FORM 1473

UNCLASSIFIED
Security Classification

UNCLASSIFIED
Security Classification

14. KEY WORDS	LINK A		LINK B		LINK C	
	ROLE	WT	ROLE	WT	ROLE	WT
V/STOL AIRCRAFT						
DOWNWASH FLOW FIELD ANALYSIS						

INSTRUCTIONS

1. ORIGINATING ACTIVITY: Enter the name and address of the contractor, subcontractor, grantee, Department of Defense activity or other organization *(corporate author)* issuing the report.

2a. REPORT SECURITY CLASSIFICATION: Enter the overall security classification of the report. Indicate whether "Restricted Data" is included. Marking is to be in accordance with appropriate security regulations.

2b. GROUP: Automatic downgrading is specified in DoD Directive 5200.10 and Armed Forces Industrial Manual. Enter the group number. Also, when applicable, show that optional markings have been used for Group 3 and Group 4 as authorized.

3. REPORT TITLE: Enter the complete report title in all capital letters. Titles in all cases should be unclassified. If a meaningful title cannot be selected without classification, show title classification in all capitals in parenthesis immediately following the title.

4. DESCRIPTIVE NOTES: If appropriate, enter the type of report, e.g., interim, progress, summary, annual, or final. Give the inclusive dates when a specific reporting period is covered.

5. AUTHOR(S): Enter the name(s) of author(s) as shown on or in the report. Enter last name, first name, middle initial. If military, show rank and branch of service. The name of the principal author is an absolute minimum requirement.

6. REPORT DATE: Enter the date of the report as day, month, year, or month, year. If more than one date appears on the report, use date of publication.

7a. TOTAL NUMBER OF PAGES: The total page count should follow normal pagination procedures, i.e., enter the number of pages containing information.

7b. NUMBER OF REFERENCES: Enter the total number of references cited in the report.

8a. CONTRACT OR GRANT NUMBER: If appropriate, enter the applicable number of the contract or grant under which the report was written.

8b, 8c, & 8d. PROJECT NUMBER: Enter the appropriate military department identification, such as project number, subproject number, system numbers, task number, etc.

9a. ORIGINATOR'S REPORT NUMBER(S): Enter the official report number by which the document will be identified and controlled by the originating activity. This number must be unique to this report.

9b. OTHER REPORT NUMBER(S): If the report has been assigned any other report numbers *(either by the originator or by the sponsor)*, also enter this number(s).

10. AVAILABILITY/LIMITATION NOTICES: Enter any limitations on further dissemination of the report, other than those imposed by security classification, using standard statements such as:

(1) "Qualified requesters may obtain copies of this report from DDC."

(2) "Foreign announcement and dissemination of this report by DDC is not authorized."

(3) "U. S. Government agencies may obtain copies of this report directly from DDC. Other qualified DDC users shall request through _____."

(4) "U. S. military agencies may obtain copies of this report directly from DDC. Other qualified users shall request through _____."

(5) "All distribution of this report is controlled. Qualified DDC users shall request through _____."

If the report has been furnished to the Office of Technical Services, Department of Commerce, for sale to the public, indicate this fact and enter the price, if known.

11. SUPPLEMENTARY NOTES: Use for additional explanatory notes.

12. SPONSORING MILITARY ACTIVITY: Enter the name of the departmental project office or laboratory sponsoring *(paying for)* the research and development. Include address.

13. ABSTRACT: Enter an abstract giving a brief and factual summary of the document indicative of the report, even though it may also appear elsewhere in the body of the technical report. If additional space is required, a continuation sheet shall be attached.

It is highly desirable that the abstract of classified reports be unclassified. Each paragraph of the abstract shall end with an indication of the military security classification of the information in the paragraph, represented as *(TS), (S), (C), or (U)*.

There is no limitation on the length of the abstract. However, the suggested length is from 150 to 225 words.

14. KEY WORDS: Key words are technically meaningful terms or short phrases that characterize a report and may be used as index entries for cataloging the report. Key words must be selected so that no security classification is required. Identifiers, such as equipment model designation, trade name, military project code name, geographic location, may be used as key words but will be followed by an indication of technical context. The assignment of links, rules, and weights is optional.